Biomass and Bioenergy 159 (2022) 106406

Contents lists available at ScienceDirect

Biomass and Bioenergy

journal homepage: www.elsevier.com/locate/biombioe

Carbon dioxide removal potential from decentralised bioenergy with carbon capture and storage (BECCS) and the relevance of operational choices

Alberto Almena [*], Patricia Thornley, Katie Chong, Mirjam Röder

Energy & Bioproducts Research Institute, College for Engineering & Physical Science, Aston University, Aston Triangle, Birmingham, B4 7ET, United Kingdom

ARTICLE INFO

Keywords:
BECCS
Carbon dioxide removal
LCA
Decarbonisation of energy supply

ABSTRACT

Bioenergy with carbon capture and storage (BECCS) technology is expected to support net-zero targets by supplying low carbon energy while providing carbon dioxide removal (CDR). BECCS is estimated to deliver 20 to 70 $MtCO_2$ annual negative emissions by 2050 in the UK, despite there are currently no BECCS operating facility. This research is modelling and demonstrating the flexibility, scalability and attainable immediate application of BECCS. The CDR potential for two out of three BECCS pathways considered by the Intergovernmental Panel on Climate Change (IPCC) scenarios were quantified (i) modular-scale CHP process with post-combustion CCS utilising wheat straw and (ii) hydrogen production in a small-scale gasifier with pre-combustion CCS utilising locally sourced waste wood. Process modelling and lifecycle assessment were used, including a whole supply chain analysis. The investigated BECCS pathways could annually remove between −0.8 and −1.4 $tCO_2e\ t_{biomass}^{-1}$ depending on operational decisions. Using all the available wheat straw and waste wood in the UK, a joint CDR capacity for both systems could reach about 23% of the UK's CDR minimum target set for BECCS. Policy frameworks prioritising carbon efficiencies can shape those operational decisions and strongly impact on the overall energy and CDR performance of a BECCS system, but not necessarily maximising the trade-offs between biomass use, energy performance and CDR. A combination of different BECCS pathways will be necessary to reach net-zero targets. Decentralised BECCS deployment could support flexible approaches allowing to maximise positive system trade-offs, enable regional biomass utilisation and provide local energy supply to remote areas.

1. Introduction

Anthropogenic climate change with the sharp rise in atmospheric concentrations of greenhouse gases (GHG) is one of the biggest challenges of our time. Carbon dioxide (CO_2) is the primary GHG contributing to more than 80% of the total emissions [1]. As a result, many countries, including the United Kingdom, have adopted net-zero emissions targets to maintain global average temperature rise below 2 °C with respect to the pre-industrial era [2,3].

Since mitigation efforts are unlikely to result in the required emission reductions to prevent climate change [1], net-negative emission technologies (NETs) are increasingly discussed as a possible solution to balance GHG emission sources and sinks with the potential to offset the 'overshooting' atmospheric CO_2 concentration [4,5]. Among NETs, bioenergy with carbon capture and storage (BECCS) is an option that could generate negative emissions whilst simultaneously producing renewable energy [6]. BECCS systems create a negative carbon flow from the atmosphere into geological storage (see Fig. 1.). Carbon dioxide removal (CDR) is performed via biological sequestration during biomass growth [7]. The biomass can be used as a fuel, or it can be converted into an energy vector through the application of heat, chemicals, microbial activity or a combination of these methods [8]. However, biomass-to-energy processes can still constitute large point sources of CO_2 previously sequestered during biomass growth. Therefore, carbon capture technologies, already implemented for the fossil fuel industry [9–11], could be integrated with bioenergy processes to reduce emissions of biogenic CO_2 back to the atmosphere [12]. The captured CO_2 can be stored in appropriate geological underground reservoirs or be used for other purposes with a long-term lock-in or storage of CO_2 [13].

The potential for BECCS to deliver negative emissions does not only lie in the CDR opportunity. Modern bioenergy applications can use different biomass sources to produce heat, electricity, transport fuels or

---

* Corresponding author.
E-mail address: a.almena@aston.ac.uk (A. Almena).

https://doi.org/10.1016/j.biombioe.2022.106406
Received 8 November 2021; Received in revised form 23 February 2022; Accepted 24 February 2022

other energy carriers like hydrogen. A wide variety of commercially demonstrated bioenergy technologies could be integrated with BECCS. Potential sources of bioenergy feedstock include woody and lignocellulosic energy crops (e.g. willow, poplar, miscanthus and switchgrass), starch-containing crops (e.g. corn, wheat, potatoes), aquatic plants (e.g. algae), wood and agricultural residues (e.g. forest residues, straw), municipal solid wastes, used cooking oils, animal manure, sewage sludge and other biological resources [5,14]. Depending on the characteristics of the feedstock, the most suitable conversion pathway to bioenergy –i.e. thermochemical, biochemical or chemical– could be selected [15].

The advantages and CDR potential encompassed in BECCS have made it the dominating NET in the integrated assessment models (IAMs) of the Intergovernmental Panel on Climate Change (IPCC) [16,17]. BECCS is an essential part of most modelling pathways that limit global warming to 1.5 °C, projecting removal of between 151 and 1191 Gt CO_2 globally over the 21st century from 2020 onwards [18]. These ambitions correspond to removing an average of 13.5 $GtCO_2$ per year [19], equivalent to one-third of the global CO_2 emissions reported for 2019 [1]. In a UK climate change mitigation framework, BECCS is also expected to help achieve the net-zero emissions target by 2050 [20]. As estimated, BECCS could deliver 20 to 70 Mt CO_2 annual negative emissions for the UK [21,22].

Previous research has identified high uncertainty for the optimistic assumptions in IAMs for large scale BECCS deployment [4,23,24]. Biomass energy is widely used but not at large scale, and CCS technologies have been demonstrated but not commercially established [25]. BECCS applications are still in development, and yet the commercial experience is scarce. Six active BECCS facilities operate worldwide, capturing approximately 1.7 Mt CO_2 per year [26,27]. The only large-scale facility (>400 kt CO_2 p.a. stored) is the Illinois Industrial CCS, capturing up to 1 Mt CO_2 annually, while the remaining applications are pilot-to small-scale systems [26]. In the UK, only Drax has implemented two BECCS pilot facilities with a potential removal capacity of 700 t CO_2 p.a [28].

Since commercial BECCS deployment still requires time to be an established reality, a decentralised vision could represent a solution to enable quicker uptake of BECCS supporting CDR and local energy provision. Bioenergy processes allow scalability [29], and BECCS could integrate with existing bioenergy systems at various scales, such as modular CHP systems or gasifiers [30,31]. This would allow decentralised, demand-focused energy provision and the use of regionally sourced biomass and residues simultaneously, thus offering flexibility and sustainability benefits beyond CDR and energy supply [32]. While this might not support the classical concept of 'economy of scale', further advantages involve lower capital cost per facility and therefore a reduced risk for investors, a higher and faster industrial learning and better adaptability to market conditions [33]. In addition, the developing CO_2 utilisation market could encourage the circular carbon economy [34]. Depending on the purity of the CO_2 captured, its uses include the food and drink industry [35], the production of chemicals (e. g. methanol [36], urea [37] or polymers [38]), microalgae cultivation [39], concrete production [40], synthesis of alternative energy products (e.g. dimethyl carbonate and dimethyl ether [41]) or fire suppression [42] among others. Due to the current lack of infrastructure for CO_2 geological storage, the highly pure CO_2 captured and stored in small scale facilities could be sold as a commodity to those industries. This could generate extra revenue to support decentralised and small-scale BECCS deployment, until a centralised large-scale BECCS deployment that includes CO_2 transport and storage/utilisation infrastructure could be fully developed to support, if required, the decentralised operating system [29].

To shed light on the uncertainties identified on BECCS capacity to deliver negative emissions, this work explored and quantified, based on coupling process modelling and lifecycle analysis methodologies, the theoretical performance and CDR potential of different decentralised BECCS systems. In addition, the outcome from this study provided a metric on how the investigated scenarios could contribute to the UK's efforts to supply low carbon energy and achieve net-zero emissions. The IPCC scenarios consider three pathways for BECCS: (a) electricity and heat generation, (b) hydrogen production, and (c) liquid fuels production [17]. The present study covered two out of three scenarios included by the IAMs for BECCS:

- Case CHP considers agricultural residues (wheat straw) used in a heat and power (CHP) facility that involve post-combustion CCS.

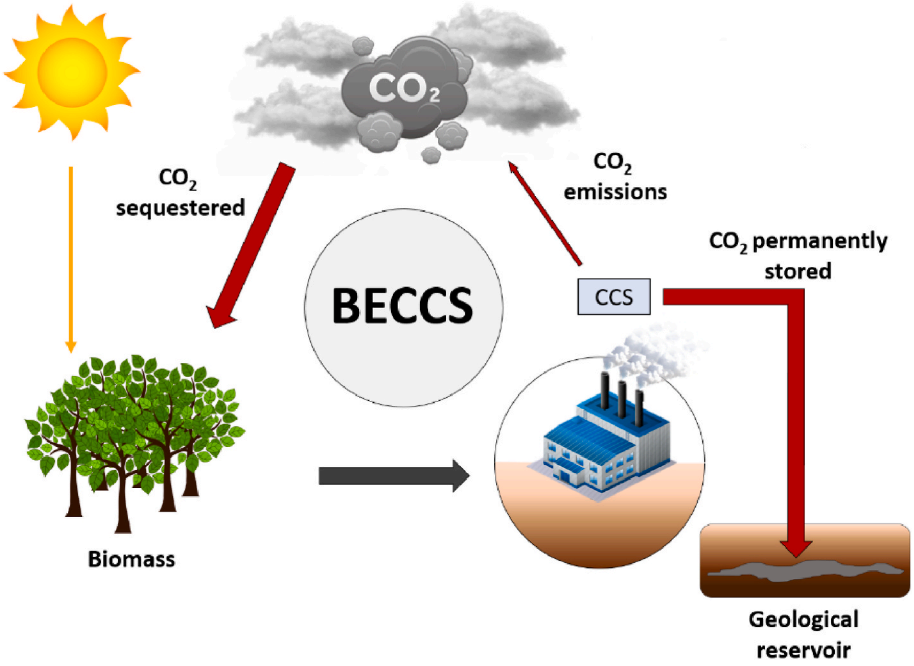

Fig. 1. The carbon flow of BECCS. When BECCS systems are employed, a negative carbon flow from the atmosphere into storage is created.

- Case H_2 considers forest residues (white pellets) used in a gasification unit to produce hydrogen, with a purity level suitable for fuel cell operation, involving pre-combustion CCS.

The objectives were to:

- Assess the lifecycle emissions and CDR potential of the two BECCS case studies to evaluate the emission impacts and benefits and their potential contribution to the UK's net-zero target.
- Assess different key performance indicators of the BECCS system and the impact of changes in the market strategy and energy demand, e.g. opt for maximising carbon sequestration or energy production. This will support a better understanding of how technology can be operated depending on economic and policy drivers and impacts on net-negative emissions potential.
- Investigate how decentralisation supports different policy and market strategies and how these affect the synergies between CDR potential, energy generation and sustainable biomass use. This will improve the understanding of the diversity of BECCS technologies and how different drivers can shape the operational choice.

2. Materials and methods

2.1. Assessment methods

Assessing the CDR and net emission potential of BECCS requires a supply chain perspective from growing and sourcing biomass to the storage or utilisation of CO_2 (see Fig. 2). This comprises the biogenic CO_2 embedded in the biomass and captured during the conversion process and all emissions related to land management, crop or forest management, harvest, biomass processing, storage, and transport at all supply chain stages. Additionally, the assessment includes emissions related to the biomass-to-energy conversion and CO_2 capture process and any emissions related to the transport, storage or use of the captured CO_2.

To assess the net-negative emission profile and compute the CDR potential of the investigated BECCS case studies, process modelling and lifecycle analysis (LCA) have been conducted. The modelling of the bioenergy conversion and CO_2 capture stages supports a detailed analysis of the process, sensitivity analysis and optimisation potential. Mass and energy balances, biomass-to-energy yield, carbon capture efficiency, power demand and additional technical features of the process have been computed and studied. The LCA was conducted to estimate the emission impact for all BECCS supply chain stages, as illustrated in Fig. 2. Variations of the key performance indicators (KPI) were used to test process sensitivity and evaluate the impact of these parameters on the process' net emissions score.

2.2. Description of BECCS case studies

The application of BECCS for power and heat cogeneration (Case CHP) and hydrogen production (Case H_2) comprise the two case studies evaluated in the present study (see Fig. 3). The technologies forming part of the investigated BECCS systems, e.g. combustion, gasification, post-combustion amine scrubbing, pre-combustion absorption using methanol or transport pipelines and CO_2 storage in saline aquifers, have been all commercially proven as detached technologies [43]. However, their commercial application as an integrated BECCS system is currently limited.

2.2.1. Case CHP: Combined heat and power generation with post-combustion capture

Case CHP, comprised of combined heat and power generation (CHP) with post-combustion CO_2 capture using wheat straw as biomass feedstock, is considered a key technology for achieving the UK Government's emission targets due to its potential role in decarbonising heating and power production [44]. Implementing an energy system that simultaneously produces heat and power can reduce carbon emissions by up to 30% compared to separate generation [45]. Several conversion routes are available for CHP [46], and this study focused on combustion combined with a steam cycle. The targeted capacity of this CHP plant is to produce 30 MW of electricity and 30 MW of thermal energy, thus characterising a medium-scale CHP facility suitable to be part of a decentralised energy supply scenario [47].

Wheat straw was selected as the bioenergy feedstock. Using residual biomass is recommended to achieve a sustainable bioenergy expansion that prevents negative consequences on land use [23,48–50]. According to 2017 data, about 1.7 Mt of the UK's wheat straw are currently not used and could be available for energetic use [51].

Post-combustion capture technology was selected to remove CO_2 from the flue gases produced during biomass combustion. Since the partial pressure of flue gas is close to atmospheric and CO_2 concentrations are relatively low, CO_2 absorption/stripping processes using a chemical solvent are the preferred option for flue gas treatment over physical absorption alternatives [52]. Amine scrubbing processes using

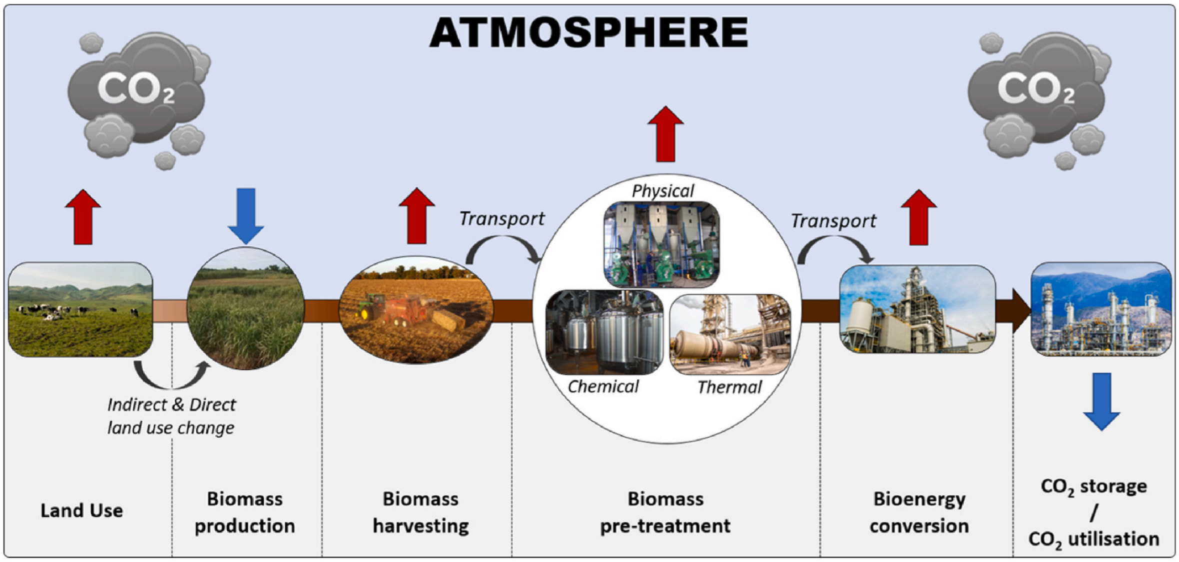

Fig. 2. BECCS supply chain. The resulting balance of CO_2 sinks (blue arrow) and sources (red arrow) will determine the net-negative emission potential of the system. (For interpretation of the references to colour in this figure legend, the reader is referred to the Web version of this article.)

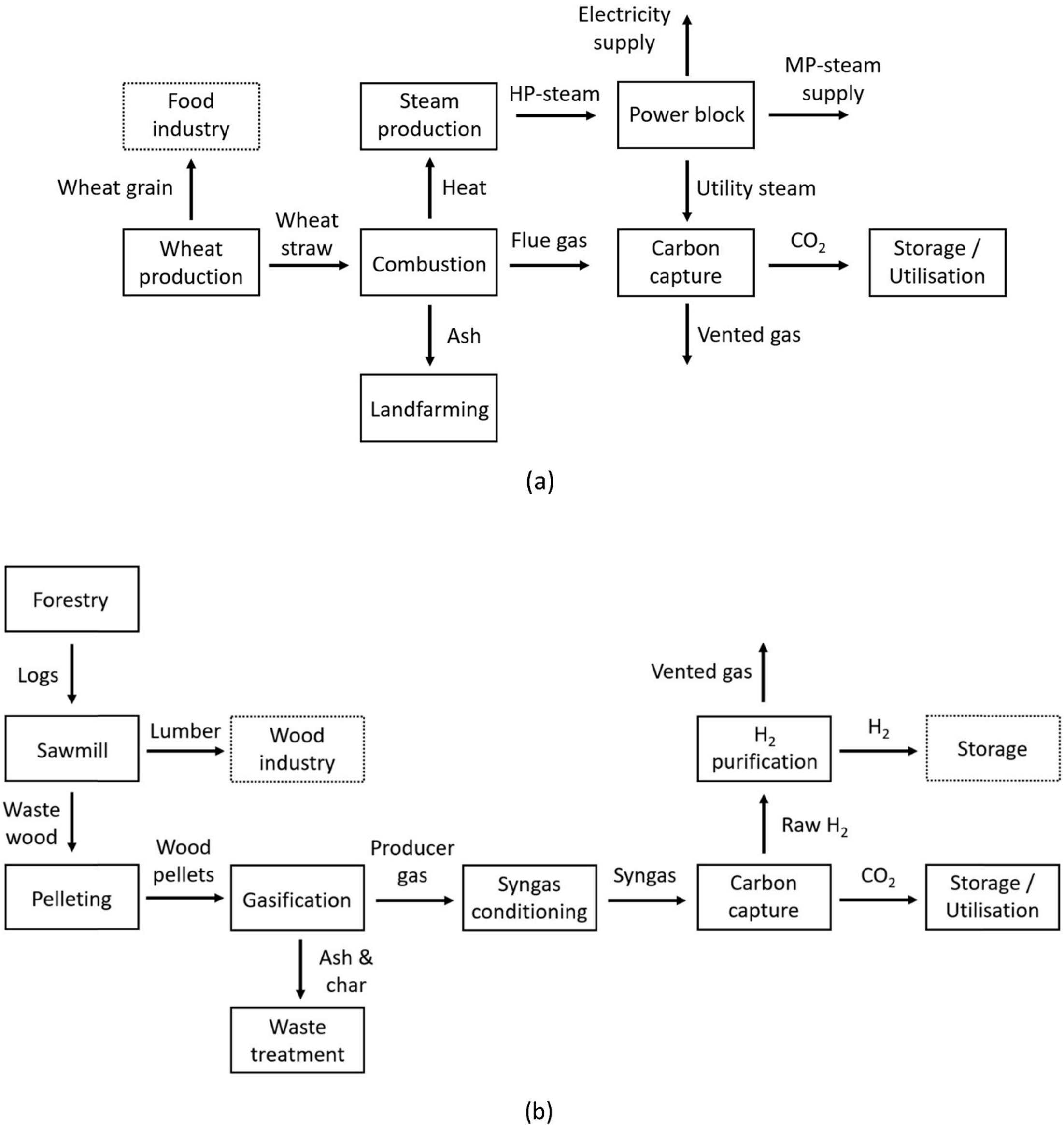

Fig. 3. Block diagram representing the two case studies assessed within this work, i.e. (a) combined heat and power generation with post-combustion CCS, and (b) hydrogen production via gasification with pre-combustion CCS. Dotted blocks are beyond the scope of the study.

aqueous solutions of alkanolamines have reached commercial application [10]. Monoethanolamine (MEA), a primary amine with high alkalinity, is an excellent choice to treat flue gases from biomass combustion since they show low CO_2 partial pressure and negligible carbonyl sulfide (COS) and carbon disulfide (CS_2) contaminants concentrations [53]. The main drawbacks of this system are the high energy intensity and corrosion involved [10,53]. On the other hand, amine scrubbing systems can recover a continuous low-pressure flow of high CO_2 concentration. For pipeline transportation and reservoir storage, the captured CO_2 stream is compressed to a supercritical fluid. The supercritical state increases the density of the fluid, and the reservoir capacity is thus enhanced [9].

2.2.2. Case H_2: Hydrogen production via gasification with pre-combustion capture

Case H_2 comprised hydrogen production via gasification with pre-combustion capture using white wood pellets from sawmill residues. Hydrogen is expected to be fundamental in the decarbonisation strategies for industry and transport to meet the UK's net-zero targets by 2050 [54–56]. In addition, hydrogen is considered a clean fuel since energy production from H_2 only results in water emissions [57,58]. Most hydrogen production processes, however, generate CO_2. Currently, fossil resources account for 96% of the primary sources of hydrogen [59], where the gasification of coal and oil fuels 48% of global hydrogen production [60]. Biomass gasification is considered a viable technology to replace fossil fuel-based hydrogen production [61,62].

As for Case CHP, and to mitigate land-use implication, a residual feedstock was considered. White wood pellets from sawmill residues were chosen as a widely available waste wood biomass feedstock. It is estimated that the UK has an availability of 16.8 Mm^3 of wood per annum over the 50 years 2013–2061 [63], of which a 30% is estimated as sawdust, offcuts and chips residue that could be used for wood pellet production [64].

A facility with a 1 MW bubbling fluidised bed (BFB) gasifier and feed rate of 300 kg h^{-1} of wood pellets were considered. This process would produce hydrogen at a quality suitable for fuel cell operation. The thermo-chemical conversion of biomass in the presence of a gasifying agent allows the production of syngas, primarily containing carbon monoxide, hydrogen, methane, and CO_2. For tar removal, a catalytic bed material (e.g. dolomite) and oil scrubber were included [62,65]. A set of ceramic filters removed the fines from the raw syngas. The concentration of hydrogen in the syngas was maximised by including two downstream water–gas shift (WGS) reactors [66]. However, using WGS for syngas conditioning also enhances CO_2 generation as a side product, and a pre-combustion capture system was incorporated to avoid venting acid gases [67]. Physical absorption methods are preferred due to the relatively high CO_2 concentration and low impact on hydrogen yield [52]. The method adopted in this study used methanol as a physical solvent for acid gases removal, a commercially proven technology (Rectisol® process) for fossil fuel pre-combustion capture [68]. The hydrogen produced in the facility is to be distributed as hydrogen fuel for utilisation in vehicular and stationary applications. According to ISO 14687:2019, a minimum fuel index with 99.97% H_2 purity is needed [69]. Therefore, a membrane system was required to meet the technical specifications to operate fuel cells [70,71]. Metal hydride technology was suggested as an option to store the produced hydrogen [72]. The captured CO_2 stream was either compressed to a liquid to enter the utilisation market or compressed to a supercritical fluid to be transported and sequestered underground.

2.3. Biomass specifications

The characteristics of the bioenergy feedstocks, wheat straw and white wood pellets assessed in the two case studies are compiled in Table 1. The proximate analysis for wheat straw was carried out on an as-received basis in the original study [73], while the data provided in Table 1 is converted to a dry basis. Wood pellets are assumed to be made from sawmill residues [74].

2.4. Process modelling

The aim of the process modelling was to perform a thermodynamic equilibrium calculation capable of predicting the thermodynamic limits of the biomass-to-energy systems. Although equilibrium is not reached under normal operation and the equipment design is not included, this type of modelling can determine the formation, consumption, and separation of those components involved in the process and set yield limits [77]. Aspen Plus was used to create a digital twin of the two case studies. Material and energy balances were performed using Aspen Plus capabilities, which include an accurate description of the physical and chemical properties of pure components and complex mixtures, together with rigorous models for the unit operations [78]. Aspen Plus was supported with Fortran user block models when required. Thus, the process modelling allowed the evaluation of plant behaviour with variations in operating conditions and performance parameters. The comprehensive report of material and energy inflows/outflows delivered by Aspen Plus was used as input for the LCA.

Table 1
Proximate and ultimate analysis data for biomass feedstock as received.

	Wheat Straw [73]	Wood pellets [74,75]
Proximate analysis (wt %, dry basis)		
Moisture	4.20[a]	6.70[a]
Volatile content (VC)	73.01	84.80
Fixed carbon	19.69	14.50
Ash	7.30	0.70
Ultimate analysis (wt%, dry basis)		
C	43.25	49.3
H	5.92	6.00
N	0.84	0.22
S	0.43	0.02
O (difference)	42.26	43.76
Low heating value (MJ kg^{-1}, dry basis)	16.41 [76]	18.73

[a] Moisture content after drying.

2.4.1. Process model case CHP: Combined heat and power generation with post-combustion capture

Fig. 4 shows process flowsheet for the CHP case study. The process model considered that the baled wheat straw was sent to a comminution stage to reach an appropriate particle size, i.e. 10 mm, for pulverised biomass combustion [79]. Due to the limitations of the software, the pulverised fuel boiler was modelled using a set of two blocks [80]. A yield reactor (RYield) was coupled with a calculator block, which converted the biomass into its 'conventional' compounds by assuming the devolatilization products can be derived from the ultimate and proximate analysis. Once the volatile components were identified, a Gibbs reactor (RGibbs) modelled the reactions assuming Gibbs free energy minimisation and chemical equilibrium. The airflow was computed to feed the stoichiometric oxygen for complete combustion to the block. A cyclone block separated solids (i.e. ash and unconverted char) from high-temperature flue gases. The heat resulting from combustion was used to produce high-pressure superheated steam (165 bar, 547 °C). Hot flue gases were used to preheat the combustion air inflow. The superheated steam flows to the steam turbine generator, which comprises a high-pressure turbine (HP-Turbine), a medium-pressure turbine (MP-Turbine) and two low-pressure turbines (LP-Turbine and AUX-Turbine). Two different low-pressure saturated steam streams were obtained from the steam turbine generator. Utility saturated steam of 3 bar (134 °C) for internal heat supply exited the LP-Turbine, while 10 bar saturated steam (180 °C) was obtained from AUX-Turbine for external heat supply. The steam leaving the MP-Turbine could bypass the low-pressure turbines and be used for internal heat supply if needed.

The CO_2-rich flue gases were subsequently expanded and blown to the amine scrubbing system. To replicate industrial size operation (solvent flow up to 455 m^3h^{-1} [53]), the absorption-desorption process was modelled using two RadFrac blocks, i.e. ABS-TOW and STRIPPER (see Section S.2 of supplementary material). A 32% MEA aqueous solution, the maximum concentration to prevent corrosion, was used as solvent [53]. NRTL electrolyte model kinetics were set to simulate the CO_2 chemical absorption (see Section S.3 in supplementary material) [81]. The absorption column head included a water washing stage (WAT-MEAW) to prevent MEA vapor release to the atmosphere. The rich solvent exiting ABS-TOW bottoms was heated and fed to the stripping column to separate the carbon dioxide and MEA. The highest heat demand was to operate the boiler from the STRIPPER block for solvent recovery. The lean solvent from the stripper's bottom was cooled, mixed with the water washing stream and recycled to ABS-TOW. The head stream with the captured CO_2 was cooled to condense part of the water content and sent to the compression block. Four compression stages with intercooling were included to reach the supercritical fluid state for CO_2.

2.4.2. Process model case H_2: Hydrogen production via gasification with pre-combustion capture

The model replicated the existing gasification pilot plant at the Energy and Bioproducts Research Institute (EBRI) at Aston University. The process flowsheet is shown in Fig. 5. Wood pellets can be readily used for gasification without any pre-processing. However, process heat surplus is used to reduce the initial moisture content to enhance the gasification performance. A bubbling fluidised bed (BFB) gasifier was operated at 800 °C and atmospheric pressure. Like combustion, gasification was modelled in Aspen Plus coupling RYield and RGibbs blocks [80]. Oxygen was supplied with an equivalence ratio (ER) of 30% reproducing biomass gasification operation [62]. It is assumed the gasification performs well without adding steam as thermal moderator [82]. Thus, no heat is required for steam production, and heat availability to supply the downstream CDR unit increases. Dolomite was used as catalytic bed material to improve heat transfer and enhance tar conversion to a gaseous product at low pressure, thus limiting the biomass tar content in the syngas [62,83]. A stoichiometric reactor block (RStoic) was added before the RGibbs to simulate tar production. Tar was assumed to be represented only by naphthalene [65], and conversion was set to allow

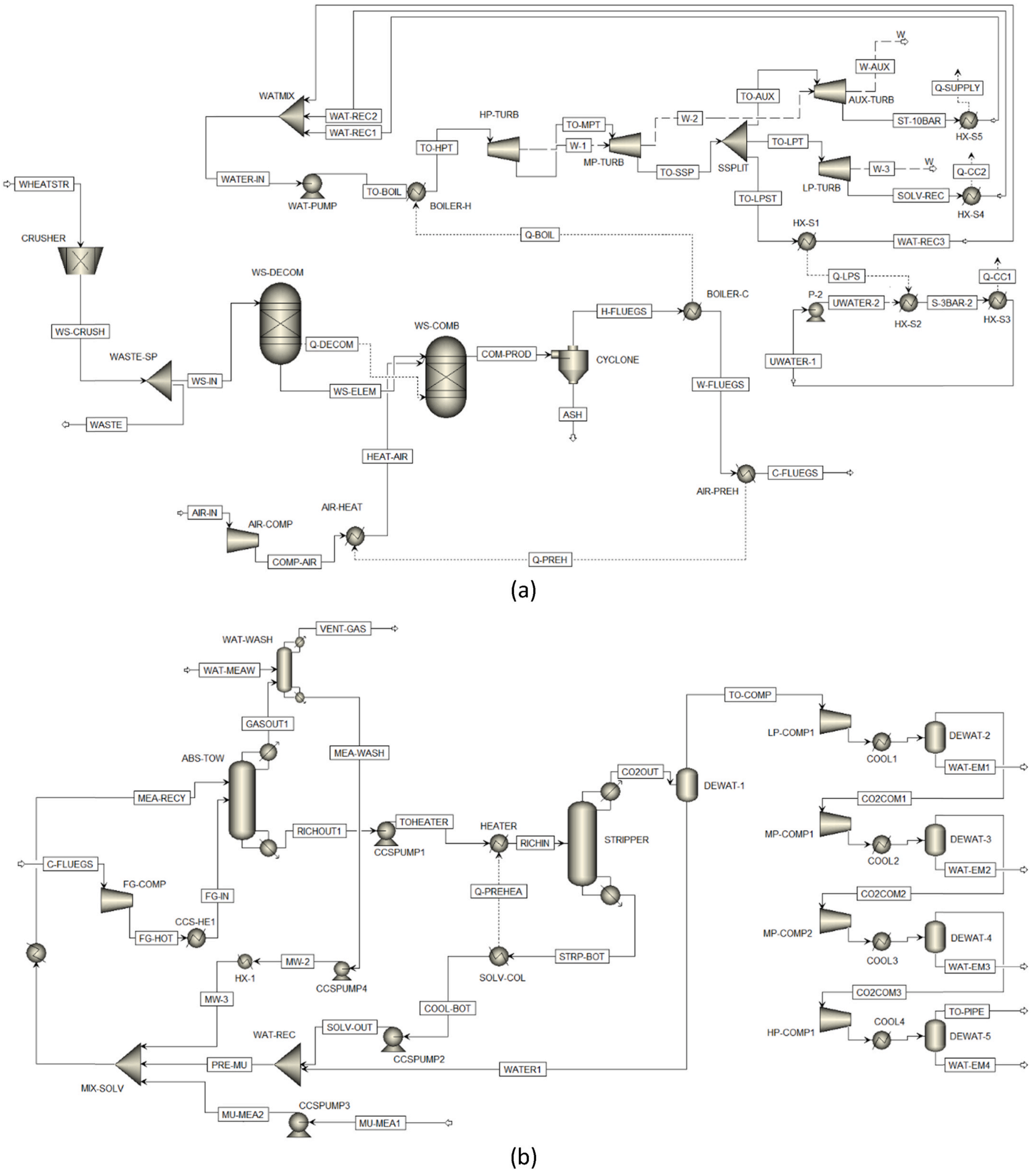

Fig. 4. Flowsheet for the wheat straw to bioenergy conversion process comprising a) CHP module and b) post-combustion carbon capture module.

2.5 g Nm^{-3} of producer gas, according to experimental data on BFB using catalytic tar reduction [84]. Ash, unconverted char and dolomite were separated from the producer gas in a subsequent cyclone. Heat was recovered from the hot gases before entering the oil scrubber for tar removal. The physical solvent, i.e. used rapeseed cooking oil, was represented in Aspen Plus by four fatty acids [85] entering the absorption column (RadFrac) at 6 °C. The Peng-Robinson equation of state with Boston-Mathias corrections was selected to predict thermodynamic properties and phase equilibrium behaviours for mixes that involve gas processing [86]. The rich solvent from the column bottoms was chilled, decanted and cleaned in a centrifuge to be recycled (cleaning system not shown in Aspen Plus model).

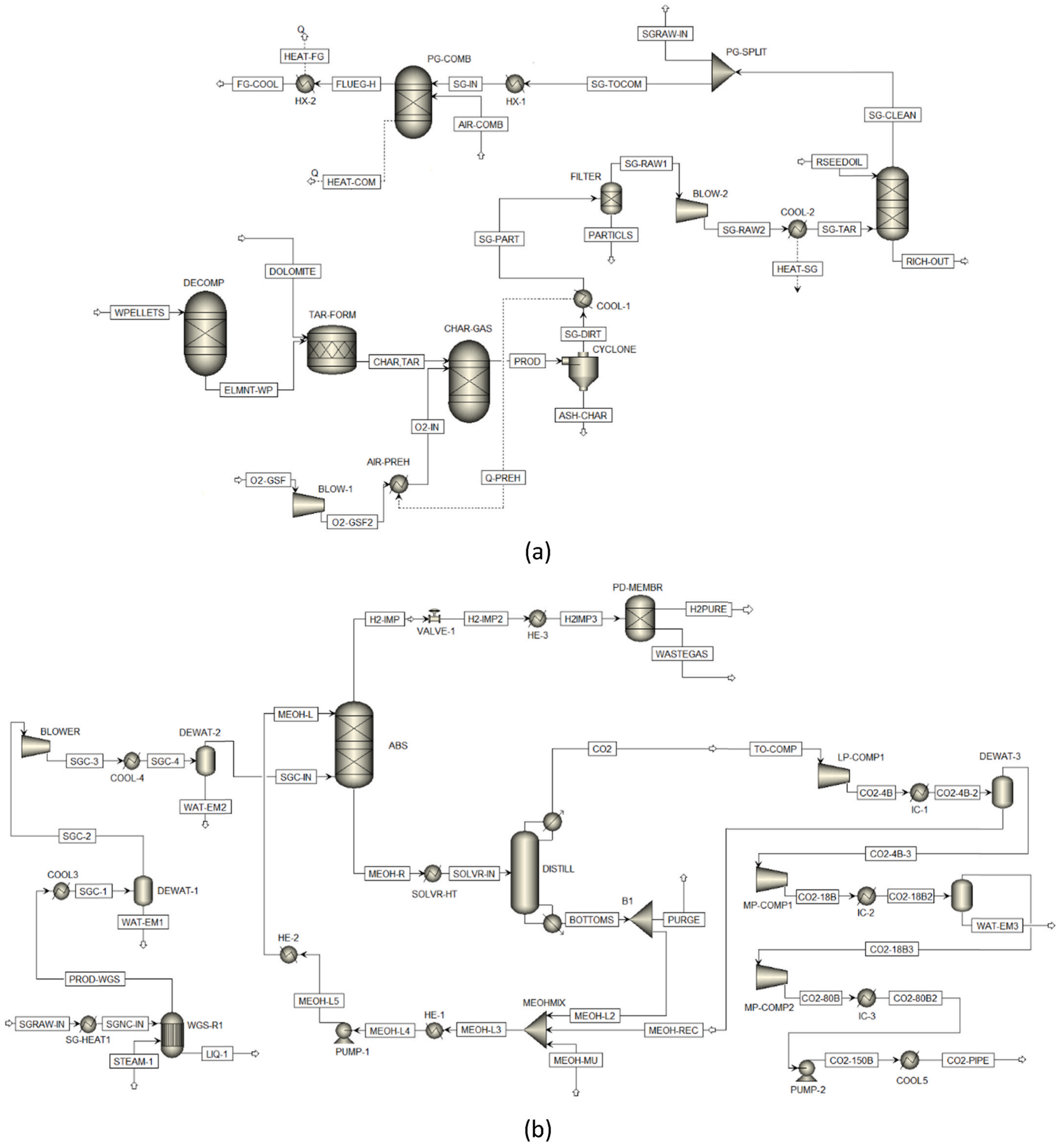

Fig. 5. Flowsheet for the waste wood conversion to hydrogen comprising a) Gasification module with tar removal and syngas combustion, and b) syngas conditioning with pre-combustion carbon capture module, hydrogen purification and CO_2 compression block.

The cleaned syngas exited the oil scrubber from the top. The main syngas stream was sent to the WGS process, while a fraction of the syngas (the percentage depends on the process heat requirements) was burned for internal heat supply. Low-temperature catalysed WGS reactions occurred in an equilibrium reactor block (REquil) at atmospheric pressure and 132 °C. A calculator block was programmed to feed a steam/CO ratio of 1:1 to the reactor, thus enhancing the forward reaction to hydrogen [87]. The conditioned syngas was next cooled down and flashed (Flash2) for water removal before compression. The Rectisol system operates at sub-ambient temperatures and medium pressures for efficient physical absorption of acid gases in methanol. The absorption column (RadFrac) feed stream was syngas previously compressed to 30 bar and cooled to -21 °C, and methanol solvent at -30 °C [68]. A reverse Carnot cooling cycle using ammonia as a refrigerant (R717) was assumed to reach temperatures at standard conditions. The coefficient of performance (COP), defined as the ratio of the evaporator load to the power consumed by the compressor, for ammonia evaporating at −40 °C (0.07 MPa) and condensing at 25 °C (1 MPa) was 2.15, and the Carnot efficiency was assumed to be a 60% [88,89]. Rich solvent exited the absorption tower at the bottoms to be heated and sent to a distillation column (RadFrac). Lean solvent was extracted from the boiler, mixed with the make-up methanol stream and recycled. CO_2 was obtained from the partial-vapor condenser and sent to the compression stage as described for Case CHP.

The gaseous headstream, mainly containing hydrogen, was sent to the purification stage. The pressure was enough to be expanded, operate a membrane system (modelled as a separation block with experimental yields [90]) to reach fuel cell application purity [91] and be stored in metal hydrides. Low pressure (10–20 bar) and ambient temperatures are enough for this hydrogen storage technology [92,93]. Since hydrogen suitable for fuel cell operation is produced, the internal power supply was assumed to be satisfied using stacked PEM fuel cell technology (up to 250 KW), operated by a fraction of the produced hydrogen flow. The fraction of syngas burned for energy supply, and thus the associated CO_2 emissions (in this process no post-combustion CCS is considered), were reduced.

2.5. Life cycle assessment

The goal of the LCA was to evaluate climate change impacts, i.e. CO_2 and CO_2 equivalents, of the investigated case studies. The functional unit was defined as '1 MWh of energy delivered by the process'. According to this definition, for the CHP process, the cogeneration of 1 MWh of heat and electricity was considered. For the hydrogen production process, the product mass flow equivalent to 1 MWh of useable energy was accounted. Hydrogen free Gibbs energy (33.33 kWh kg^{-1}), i.e. the maximum amount of useable energy available when hydrogen recombines with oxygen [95], was used to convert hydrogen mass flow into an energy equivalent. The corresponding unit of measurement was, therefore, kg of CO_2 equivalents per MWh produced. Both biogenic and fossil CO_2 emissions and additional GHG releases to the atmosphere were accounted for. An attributional LCA with a cradle-to-grave perspective was performed [94]. Mid-point characterisation modelling was applied since evaluating the latest implications at the cause-effect chain is beyond the scope of this work [95]. The LCA followed ISO 14040/44 standards and was performed in SimaPro® 9.1. The lifecycle impact assessment (LCIA) method used was the ILCD 2011 Midpoint + V1.11 to classify and characterise climate change impacts and estimate the resulting net airborne emissions of the system [96].

The system studied here is illustrated in Fig. 6. The system boundaries comprised the whole supply chain, including biomass production, harvest, transportation, feedstock pre-treatment, biomass-to-energy conversion, CO_2 capture, transport and storage. Accounting for the emissions associated with the utilisation of the captured CO_2 was not within the scope of this research. The average environmental burdens from those stages to produce a nominated functional unit were obtained from Ecoinvent 3.6. The process modelling provided the data for assessing the bioenergy conversion stage with carbon capture. Data to evaluate the transport and storage of CO_2 was taken from García-Freites, Gough and Röder [97].

The two case studies used residual biomass resources; hence no land-use change implications were included. Instead, biomass supply chain emissions from land establishment to arrival at the bioenergy plant were computed by adapting existing Simapro modules, 'Wheat straw, at farm/ UK Mass' included in Agri-footprint database and 'Wood pellets at storehouse' for a European framework included in Ecoinvent 3.6 database.

The wheat straw module was adapted to allocate the environmental impacts from wheat production to the wheat straw by-product on a dry matter basis (39%). It was assumed wheat straw were dried naturally before being packed in bales and transported to the facility. Additionally, CO_2 sequestration during biomass growth and transport of the straw bales over a distance of 100 km (roundtrip) from the farm to the bioenergy plant [73] were included in the assessment. The white wood pellets module was used without further addition since it included the associated CO_2 sequestration, transport and pelleting.

When more than one type of energy is produced, i.e. CHP scenario, an exergy-based allocation was applied to partition inputs and outputs [98,99]. Downstream emissions associated with supercritical CO_2 transportation and underground injection were obtained from previous work [97].

The oxygen supplied to perform wood pellet gasification in Case H_2 was assumed to be supplied by a cryogenic air separation unit (not part of process modelling). Therefore, oxygen production and supply emissions were considered within the LCA boundaries and calculated using Simapro module 'Oxygen, via cryogenic air separation, production mix, at plant, gaseous EU-27 S'.

Green methanol was assumed to be produced externally and was used as a solvent for the Rectisol system [100]. Therefore, the existing Simapro model 'Methanol, from biomass/RoW' was considered. A

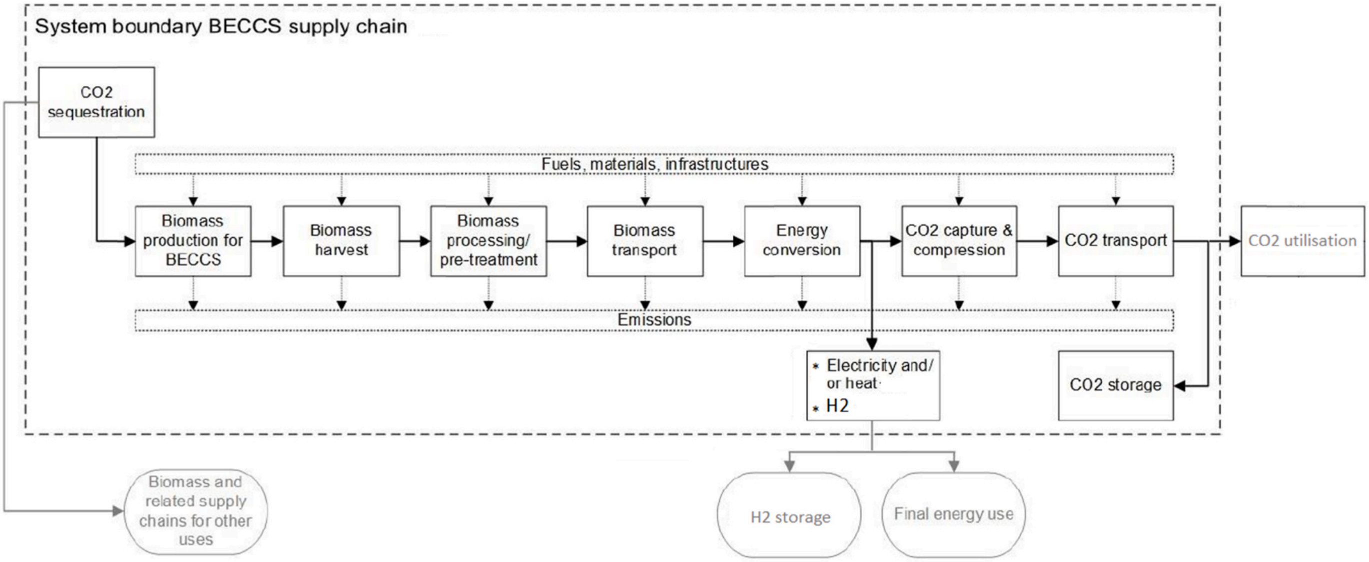

Fig. 6. System boundary for BECCS supply chain within this study.

negative emissions contribution is expected from using this type of methanol, which was included within the energy conversion block.

Although metal hydride technology has been identified as a suitable option to store the produced hydrogen, hydrogen storage was considered beyond the LCA boundaries for Case Study B.

2.6. Variation in net-emission potential from alternative operation modes

This analysis assessed the variations of the net-emissions score for the investigated case studies when considering different KPI and thus evaluated alternative operational strategies for the same technology. A more detailed description and justification of the scenarios assessed here can be found in Section S.1 of the supplementary material.

The CHP operation baseline scenario targeted 30 MWe and 30MWth supply while removing the maximum ratio of CO_2 possible without external energy inputs. In addition, five alternative scenarios comprising different operational settings for Case Study A were considered:

- Scenario CHP.1 looked at supplying and maximising electricity production to represent the strategy that would provide the highest revenue for the operator. A standard efficiency of 72% (80% isentropic efficiency and 90% mechanical efficiency) for the turbine was considered [101], such as for the benchmark scenario. Efficiencies of steam turbines, however, can vary and range from 40% to 90% of an ideal turbine yield [102].
- Scenario CHP.2 assumed ideal turbine operation to compute the system's theoretical maximum electricity production and assess how improving turbine efficiency can affect the CDR removal potential.
- Scenario CHP.3 represented a strategy that prioritises carbon capture yield at the expense of energy supply, which could be preferable when revenue is linked to emission offsets.
- Scenarios CHP.4 (i) and (ii) evaluate the uncertainty in the carbon capture system energy requirements. Previous studies that used the same post-combustion technology considered here reported energy consumptions between 10.3 (deficient operation) and 4.1 GJ (optimal operation) per tonne of CO_2 captured [103–105].

For Case Study B, the baseline operation mode considered oxygen for the gasification agent and targeted maximum carbon capture yield. In addition, five alternative scenarios including different operational settings were considered:

- Scenario H_2.1 assessed how the process would perform using air as a gasification agent, thus replicating the EBRI pilot plant operation.
- Scenario H_2.2. limits the solvent flow so that the Rectisol capture rate decreased to 70%, thus achieving the efficiency reported in most industrial processes [68].
- Scenarios H_2.3. relates to current uncertainties in fuel cell technologies performance, three alternative electricity sources were considered for powering the plant, such as (i) including a hydrogen CHP module in the process, (ii) taking it from the UK grid, or (iii) power-to-gas approach using renewable energy (wind power).

3. Results

3.1. Process modelling

The technical assessment results of the bioenergy conversion and CO_2 capture stages of the two case studies are presented in Table 2. The mass and energy balances for the two benchmark case studies are shown in Section S.4 of supplementary material.

For Case CHP, 58 t h^{-1} of biomass was required to produce 30 MW of electricity and 30 MW of heat (38.35 t h^{-1} of 10 bar saturated steam). The energy conversion efficiency was 23% with respect to the biomass energy content on a dry basis (16.41 MJ kg^{-1}). Gross electricity generation in the CHP block was 41.6 MWe, sufficient to power the whole process and reach the production target. A thermal energy surplus of 133.98 t h^{-1} of 3 bar saturated steam was generated and used to remove 78% of the CO_2 content from the flue gases. To achieve that, 455.22 t h^{-1} of 32 w% MEA aqueous solution was fed to each absorption column and recovered at the coupled stripping column. The cogenerated utility steam was used to operate the two boilers. The uncondensed water in the gaseous CO_2-rich stream that exited the absorption-desorption closed-cycle was balanced with a water washing and water make-up stream to maintain MEA concentration and prevent corrosion. The joint compression block processed the two CO_2 streams producing 68.36 t h^{-1} of highly pure (99.8%) supercritical CO_2. The emissions associated with the bioenergy conversion process accounted for 19.65 t h^{-1} of biogenic CO_2 released to the atmosphere.

Table 2
Technical performance of biomass-to-energy processes.

Parameters	Case CHP – Wheat straw CHP	Case H_2 – Hydrogen from waste wood
Biomass input (kg h^{-1})	58,000	300
Biomass energy content (MW)	264.45[a]	1.56[a]
Net power output (MWe)	30.2	0.42[b]
Net heat output (MWth)	30.2	–
Internal power supply (MWe)	11.4	0.23
Internal heat supply (MW)	165.1	0.43
Energy efficiency (dry basis)	23%	27%
CO_2 capture rate at CCS unit	78%	98%
Net CO_2 removal	78%	81%
CO_2 captured per unit of energy produced (kg CO_2 MWh^{-1})	1131	1033
Captured CO_2 concentration (w %)	99.8%	99.0%
Airborne CO_2 emissions per unit of energy produced (kg CO_2 MWh^{-1})	326	181

[a] Computed using biomass low heating value.
[b] Computed using hydrogen-free Gibbs energy, i.e. maximum yield to electricity.

For Case H_2, results showed that gasifying 300 kg h^{-1} of wood pellets resulted in a production rate of 12.6 kg h^{-1} of hydrogen suitable for fuel cell operation (99.97% of hydrogen content). The energy content of the product stream was 0.42 MWe considering hydrogen-free Gibbs energy (33.33 kWh kg^{-1}). Using 1.77 m^3h^{-1} of methanol, the pre-combustion CC system could remove 98% of the CO_2 content from the syngas. A flow of 439 kg h^{-1} CO_2 with high purity (99.0%) was recovered, compressed for pipeline transport and storage. The heat requirements not satisfied with heat recovery from the hot process streams (e.g. hot producer gas out of the gasifier) were met by burning a fraction (14%) of the producer gas. The power requirements for the cooling process of the solvent were satisfied using 9.7 kg h^{-1} of the produced hydrogen to operate a stacked PEM fuel cell with an estimated electrical efficiency of 60% [106,107]. Since no post-combustion CC was included here, flue gases from the producer gas combustion and the waste gas from the membrane unit containing CO_2 were vented to the atmosphere. The carbon emissions of the process resulted in 76.18 kg h^{-1} of biogenic CO_2.

The recovered CO_2 was highly pure in the two scenarios (>99.0%), which offers potential for utilisation instead of storage [108]. That level of purity makes the captured CO_2 suitable for carbonated beverages, enhanced gas/oil recovery, synthesis of chemicals (methanol, methane, urea), and polycarbonates, algae cultivation, refrigeration, metal casting, coffee decaffeination or mineral carbonation [109].

3.2. Life cycle assessment

Following the methodology described in Section 2.4, the LCA results present the net GHG emissions carbon dioxide mass equivalents produced per unit of energy (kg CO_2e MWh^{-1}) of the two case studies (see Table 3). The LCA inventory can be consulted in Section S.5 within the supplementary information. The supply chain emissions have been

Table 3
Carbon attribution per stage for the investigated BECCS case studies.

	Case CHP: Wheat straw to CHP with post-combustion CCS	Case H_2: Wood pellets to H_2 with pre-combustion CCS
CO_2 biological sequestration *(kg CO_2e MWh^{-1})*	−1474	−1277
Emissions – Biomass supply chain *(kg CO_2e MWh^{-1})*	361	123
Emissions – Bioenergy conversion *(kg CO_2e MWh^{-1})*	348	275
Emissions – CCS Infrastructure *(kg CO_2e MWh^{-1})*	22	20
Net emissions *(kg CO_2e MWh^{-1})*	−743	−859

merged and classified into four categories, i.e. CO_2 uptake during biomass growth, CO_2 emissions from the bioenergy feedstock supply chain, the bioenergy conversion with CC facility, and the CCS infrastructure operation. The resulting net emission flow is also presented.

Results showed that for Case CHP, biomass growth sequestered −1474 kg CO_2e from the atmosphere per MWh later produced at the CHP facility. Biomass supply chain including land management, biomass processing and transportation accounted for 361 kg CO_2e MWh^{-1}. This contribution was similar to the CO_2 emissions associated with the bioenergy conversion stage (348 kg CO_2e MWh^{-1}). Transporting the captured CO_2 through pipelines and operating the geological storage infrastructure accounted for 22 kg CO_2e MWh^{-1}. As a result, Case CHP system delivered −743 kg CO_2e net-negative emissions per MWh produced.

Case H_2 supply chain also resulted in net-negative emissions. 1 MWh supplied by the hydrogen produced by the BECCS system offset −859 kg of atmospheric CO_2. The required biomass sequestered −1277 kg CO_2e MWh^{-1} during its growth, while the CO_2 emissions accounted for 123 kg CO_2e MWh^{-1}, 430 kg CO_2e MWh^{-1} and 20 kg CO_2e MWh^{-1} for the feedstock supply chain, bioenergy conversion stage and CCS infrastructure, respectively.

3.3. *Evaluation of alternative technical configurations*

3.3.1. *Case CHP alternative operation*

Tables 4 and 5 present the process modelling and LCA results of the alternative operation analysis for Case CHP. KPI operating the CHP facility were changed, resulting in different performance parameters and emission profiles.

Scenario CHP.1 presents electricity only production. 39 MW of net electricity was generated from 58 t h^{-1} of wheat straw. The co-produced heat (252.00 t h^{-1} of 3 bar saturated steam) was used entirely for internal heat supply, so the CO_2 capture system could be enhanced to remove 87% of the CO_2 from the flue gases. As a result, 76 t h^{-1} of CO_2 was captured and stored, while 12 t h^{-1} of biogenic CO_2 was released to the atmosphere resulting in −1362 kg CO_2e MWh^{-1} net-negative emissions.

Scenario CHP.2 presents ideal turbine operation, leading to a theoretical maximum net electricity production of 59 MW. The heat allowed the removal of 71 t h^{-1} of CO_2 (82%) from the flue gases, while 16 t h^{-1} CO_2 were released. The CDR potential was −817 kg CO_2e MWh^{-1}.

If the operator prioritises carbon capture yield, i.e. Scenario CHP.3, and increases the CO_2 capture to remove 95% of the CO_2 from flue gas, 83 t h^{-1} CO_2 were captured and stored, 4.5 t h^{-1} CO_2 were emitted to the atmosphere. This Scenario had the highest CDR potential, i.e. −2721 kg CO_2e MWh^{-1}, but the energy produced was reduced to 22 MW of electricity.

Table 4
Technical performance of Case CHP biomass-to-energy process when considering alternative KPI scenarios.

Parameters	CHP.1 *(max. electricity)*	CHP.2 *(ideal turbine)*	CHP.3 *(max. CC)*	CHP.4 (i) *(max. CC – 81% energy demand)*	CHP.4 (ii) *(max. CC – 47% energy demand)*
Biomass input (kg h^{-1})	58,000	58,000	58,000	58,000	58,000
Biomass energy content (MW)	264.45[a]	264.45[a]	264.45[a]	264.45[a]	264.45[a]
Net power output (MWe)	38.58	59.31	21.92	30.02	32.55
Net heat output (MWth)	-	-	-	30.46	95.14
Internal power supply (MWe)	12.22	9.16	13.04	13.04	13.04
Internal heat supply (MW)	184.38	174.12	202.57	163.11[b]	95.63[b]
Energy efficiency (dry basis)	14.59%	22.43%	8.29%	22.87	48.29
CO_2 capture rate at CCS unit Carbon Capture unit efficiency	87%	82%	95%	95%	95%
Net CO_2 removal	87%	82%	95%	95%	95%
CO_2 captured per unit of energy produced (kg CO2 MWh^{-1})	1,973	1,213	3,802	1,378	660
Captured CO_2 concentration (w %)	99.8	99.8	99.8	99.8	99.8
Airborne CO_2 emissions per unit of energy produced (kg CO_2 MWh^{-1})	305	269	207	75	18

[a] Computed using biomass low heating value.

[b] Hypothetical results based on energy demands for amine scrubbing systems reported in literature.

Table 5
Carbon attribution per stage for Case CHP supply chain when considering alternative KPI scenarios.

	CHP.1 *(max. electricity)*	CHP.2 *(ideal turbine)*	CHP.3 *(max. CC)*	CHP.4 (i) *(max. CC – 81% energy demand)*	CHP.4 (ii) *(max. CC – 47% energy demand)*
CO_2 biological sequestration *(kg CO_2e MWh^{-1})*	−2305	−1499	−4057	−1470	−704
Emissions – Biomass supply chain *(kg CO_2e MWh^{-1})*	564	367	993	360	172
Emissions – Bioenergy conversion (kg CO_2e MWh^{-1})	340	292	269	86	39
Emissions – CCS Infrastructure (kg CO_2e MWh^{-1})	38	23	74	22	13
Net emissions (kg CO_2e MWh^{-1})	−1362	−817	−2721	−997	−480

The results of the previous case studies indicate that the solvent regeneration energy, estimated by Aspen, represented non-optimal operation of the amine scrubbing system within the range reported in the literature for pilot plant operation (explained in Section S.1 of supplementary material) [103–105]. Scenarios CHP.4 evaluated that uncertainty, which is related to the amount of stripping steam needed to perform the solvent recovery, and how this affects both energy production and CDR score. Scenarios CHP.4 maintained the maximum CO_2 capture ratio (95%), so in both cases, the CO_2 capture and emission rates were similar to Scenario CHP.3, i.e. 83 t h^{-1} CO_2 and 4.5 t h^{-1} CO_2, respectively. However, the net-negative emissions delivered by the system, when reported per unit of energy produced, resulted in different outcomes. When 81% of the energy demand reported by Aspen (Scenario CHP.4 (i)) was assumed, the system was capable of increasing energy supply to the benchmark case's production (30MWe and 30MWth) while removing −997 kg CO_2e MWh^{-1}. Scenario CHP.4 (ii) reduced the energy demand of the post-combustion CO_2 capture process by 47%, i.e. an optimised pilot plant operation [103]. The reported net-negative emissions were −480 kg CO_2e MWh^{-1}.

3.3.2. *Case H_2 alternative operation*

Tables 6 and 7 present the process modelling and LCA results of the alternative operation analysis for Case H_2.

Scenario H_2.1 presents the use of air as the gasification agent. 6.08 kg h^{-1} H_2 (0.20 MWe) was produced. 98% of CO_2 was removed from the syngas, i.e. capturing 412 kg h^{-1} CO_2. However, 18% of the producer gas was burned to operate the CO_2 capture unit, and 100 kg h^{-1} CO_2 was emitted. The net CO_2 removal yielded 77%, and the CDR potential was −1772 kg CO_2e MWh^{-1}.

Scenario H_2.2 used less methanol for carbon capture, and the Rectisol efficiency dropped to 70%. As a result, H_2 production increased to 15.76 kg h^{-1}, equivalent to 0.53 MWe. 8% of the producer gas was combusted for internal heat supply resulting in net CO_2 removal of 63%. As a result, 335 kg h^{-1} CO_2 was stored, while 72 kg h^{-1} CO_2 were emitted. Therefore, the net-negative emissions were −491 kg CO_2e MWh^{-1}.

Scenarios H_2.3 (i-iii) present the use of alternative power sources for the internal conversion process. Modelling a hydrogen CHP (i) resulted in the lowest hydrogen product outflow, i.e. 4.15 kg h^{-1} (0.14 MWe). Burning no producer gas and maximising the Rectisol efficiency (98%) led to 94% net CO_2 capture with 434 kg h^{-1} CO_2 stored and 8 kg h^{-1} CO_2 emitted. Due to the lowest biomass-to-energy efficiency and the highest carbon capture yield, the highest CDR potential for the Case H_2 supply chain was reported removing −3048 kg CO_2e MWh^{-1}.

Considering internal power supply from external power sources such as the UK mains (ii) or wind power (iii) increased hydrogen production to 22.33 kg h^{-1} (0.74 MWe). Using UK grid electricity resulted in −270 kg CO_2e MWh^{-1} negative emissions, and using wind power (power-to-gas approach) increased the CDR potential of the system to −478 kg CO_2e MWh^{-1}.

4. Discussion

4.1. *Comparison between case CHP and case H_2*

Fig. 7 shows a comparison of the two investigated case studies, comparing the emission profiles, net emissions and CDR potentials per unit of energy. The supply chain emissions are higher for case A, which can be explained by the use of fertiliser during wheat production causing N_2O emission and the lower bulk density of wheat straw, leading to higher transport emissions. On the other hand, even though wood pellet production requires energy during pelleting, the higher global warming potential of N_2O has a significantly higher impact than pelleting in Case H_2.

In Case CHP, the emissions related to upstream processes (biomass supply) were similar to those of the energy-conversion stage. In Case H_2, the most significant contributor to the emission profile is the conversion stage, which accounted for more than twice the emissions associated with the feedstock supply chain. The process modelling showed that pre-combustion CCS achieved a similar CO_2 capture rate (81%) to post-combustion CCS (78%). Case H_2 energy conversion also included further upstream contributions from oxygen (44 CO_2e MWh^{-1}), and make-up methanol (171 CO_2e MWh^{-1}) supplies that made the associated airborne emissions superior to those of Case CHP energy conversion. However, the lower carbon intensity of green methanol could offset part of the emissions generated from its production, i.e. −155 kg CO_2e MWh^{-1}, which allowed Case H_2 energy conversion module to report lower net emissions than the Case CHP counterpart. The emissions contributions from the construction and operation of the CCS infrastructure were one order of magnitude lower than feedstock and energy conversion results for both case studies.

Case CHP represented lower energy efficiency than Case H_2, with 23% efficiency for the wheat straw CHP and post-combustion process vs the 27% efficiency of the wood pellets gasification and pre-combustion process. Biomass requirements to produce 1 MWh were 0.96 tonnes of wheat straw for Case CHP and 0.71 tonnes of wood pellets for Case H_2. The lower biomass-to-energy yield in Case CHP entailed greater biological CO_2 sequestration, as shown in Fig. 7. However, that does not directly imply that the process is preferable. The research objective was to identify efficient and sustainable bioenergy processes capable of

Table 6

Technical performance of Case H_2 biomass-to-energy process when considering alternative KPI scenarios.

Parameters	H_2.1 *(gasification agent: air)*	H_2.2 *(CC efficiency 70%)*	H_2.3 (i) *(alternative power supply: H_2 CHP)*	H_2.3 (ii) *(alternative power supply: mains)*	H_2.3 (iii) *(power-to-gas: wind power)*
Biomass input (kg h^{-1})	300	300	300	300	300
Biomass energy content (MW)	1.56[a]	1.56[a]	1.56[a]	1.56[a]	1.56[a]
Pure hydrogen flow (kg h^{-1})	6.08	15.76	4.15	22.33	22.33
Net power output (MWe)	0.20[b]	0.53[b]	0.14[b]	0.74[b]	0.74[b]
Internal power supply (MWe)	0.32	0.23	0.26	0.23	0.23
Internal heat supply (MW)	0.50	0.32	0.45	0.43	0.43
Energy efficiency (dry basis)	13%	34%	9%	47%	47%
CO_2 capture rate at CCS unit	98%	70%	98%	98%	98%
Net CO_2 removal	77%	63%	94%	81%	81%
CO_2 captured per unit of energy produced (kg CO_2 MWh^{-1})	2030	637	3626	583	583
Captured CO_2 concentration (w %)	99.0%	99.0%	99.0%	99.0%	99.0%
Airborne CO_2 emissions per unit of energy produced (kg CO_2 MWh^{-1})	495	339	58	102	102

[a] Computed using biomass low heating value.

[b] Computed using hydrogen-free Gibbs energy, i.e. maximum yield to electricity.

Table 7
Carbon attribution per stage for Case H_2 supply chain when considering alternative KPI scenarios.

	H_2.1 *(gasification agent: air)*	H_2.2 *(CC efficiency 70%)*	H_2.3 (i) *(alternative power supply: H_2 CHP)*	H_2.3 (ii) *(alternative power supply: UK grid)*	H_2.3 (iii) *(power-to-gas: wind power)*
CO_2 waste wood sequestration *(kg CO_2e MWh^{-1})*	−2649	−1023	−3874	−722	−722
Emissions – Biomass supply chain *(kg CO_2e MWh^{-1})*	255	98	372	69	69
Emissions – Bioenergy conversion (kg CO_2e MWh^{-1})	583	422	384	372	164
Emissions – CCS Infrastructure (kg CO_2e MWh^{-1})	39	12	70	11	11
Net emissions (kg CO_2e MWh^{-1})	−1772	−491	−3048	−270	−478

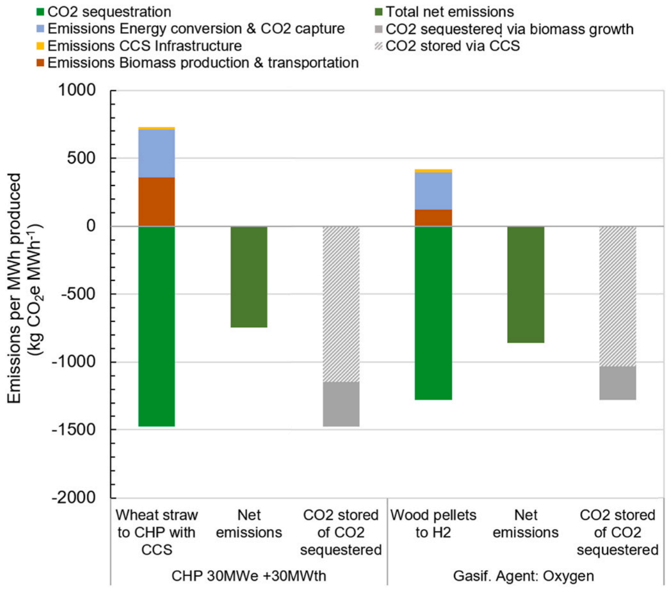

Fig. 7. GHG emissions, net emissions and CO2 storage efficiency per MWh of energy produced for the two alternative case studies, i.e. CHP (Case CHP) and Gasification (Case H_2).

delivering negative emissions. While Case CHP delivers higher carbon sequestration through the higher biomass demand, the net emissions are lower than Case H_2, making more efficient use of the biomass and having a slightly higher rate of CO_2 capture during the conversion process, as illustrated in Fig. 7.

4.2. *Case CHP alternative operation scenarios*

Fig. 8 illustrates the results for the alternative operation strategies evaluated for Case CHP, showing the energy production capacity, the net CO_2 removal ratio and net emissions of the BECCS system.

Scenario CHP.1 was operated to maximise electricity generation capacity. This increased the electricity supply by 28% compared to the Case CHP baseline. At the same time, the generated low-pressure steam was entirely used for internal processes, which allowed to enhance CO_2 removal yield from 78% to 87%. This is comparable to the modelled performances of power plants with CCS technology reported in the literature [110,111]. The captured CO_2 per energy ratio obtained, i.e. 1362 kg CO_2 MWh^{-1}, was similar to published values for biomass-fuelled CHP plants [112,113]. As a result, the net-negative emissions per MWh delivered under Scenario CHP.1 increased by 83%.

Scenario CHP.2 operated to maximise electricity generation with a more efficient turbine, increasing biomass-to-electricity yield by about 54%. Since more energy from the steam generated was converted to electricity, less heat remained available for the CO_2 removal process, which dropped to 82% but remained higher than the baseline since energy losses were minimised. The rise in electricity supply led to lower net-negative emissions per unit of energy than Scenario CHP.1, but a 10% higher value than the baseline Case CHP.

In Scenario CHP.3, the CO_2 capture rate within the CCS unit was maximised, and 95% of the CO_2 content in the flue gas was captured. More solvent was needed to reach that level of performance, and energy requirements for the solvent recovery were much higher. A 60% split fraction from the MP-turbine steam outflow was used as a utility to support the 3-bar saturated steam leaving the LP-turbine for internal heat supply. This resulted in only electricity generation with a net capacity of 21.9 MW. While the energy production dropped significantly, the net-negative emission would increase by 266% compared to the baseline, making Scenario CHP.3 the one with the highest CDR potential per unit of energy.

Scenario CHP.4 evaluated the sensitivities of the energy requirements for the CO_2 capture process. Previous studies involving pilot plant operation using the same post-combustion CCS technology as Case CHP reported energy requirements ranging between 3.6 and 4.1 GJ t^{-1} CO_2 under optimised conditions [103–105]. The primary source of uncertainty is the variation of steam requirements in the desorption column [103]. The process model results showed that about 73% of the solvent recovery energy requirements were related to stripping steam generation (6.3 Gt t^{-1} CO_2 of 8.7 GJ t^{-1} CO_2). At the same time, the remaining heat was mainly used to supply the desorption energy (2.2 Gt t^{-1} CO_2) along with solvent and reflux heating (0.2 GJ t^{-1} CO_2). Thus, compared to Mangalapally and Hasse (2011) pilot plant results, the value generated in Aspen was an unoptimized operation.

With the same CO_2 capture rate as Scenario CHP.3 (95%), Scenario CHP.4 had a significantly higher energy output and much lower net-negative emissions. The evaluation of the uncertainty related to the stripping steam requirements in Scenario CHP.4(i) showed a net capacity of 30 MWe and 30 MWth (benchmark case energy production) could be achieved when solvent recovery was performed consuming 7.0 GJ t^{-1} CO_2, i.e. an 81% of the energy initially estimated by Aspen. Since uncertainty is related to the amount of stripping steam required to perform the CO_2–solvent separation, 4.7 GJ $t^{-1}CO_2$ were used to produce stripping steam for the solvent recovery. While the energy output was the same as the baseline, Scenario CHP.4(i) led to 34% higher net-negative emissions. Scenario CHP.4(ii) considered the same energy requirements for CO_2 capture reported by Mangalapally and Hasse (2011), i.e. 4.1 GJ t^{-1} CO_2. The process model suggested that, once the rest of the energy shares were deducted, the energy requirements would be met using 1.8 GJ t^{-1} CO_2 to produce stripping steam, which is a 28% of the steam flow initially estimated Aspen to perform the CO_2–solvent separation. This would result in a much higher biomass-to-energy efficiency for the process (more heat is available for customers) and, consequently, the lowest net-negative emissions per unit of energy delivered (−482 kg CO_2e MWh^{-1}) from the investigated scenarios was obtained.

The metric commonly used to compute the GHG emissions associated with a particular energy vector is the energy-specific emissions factor, i.

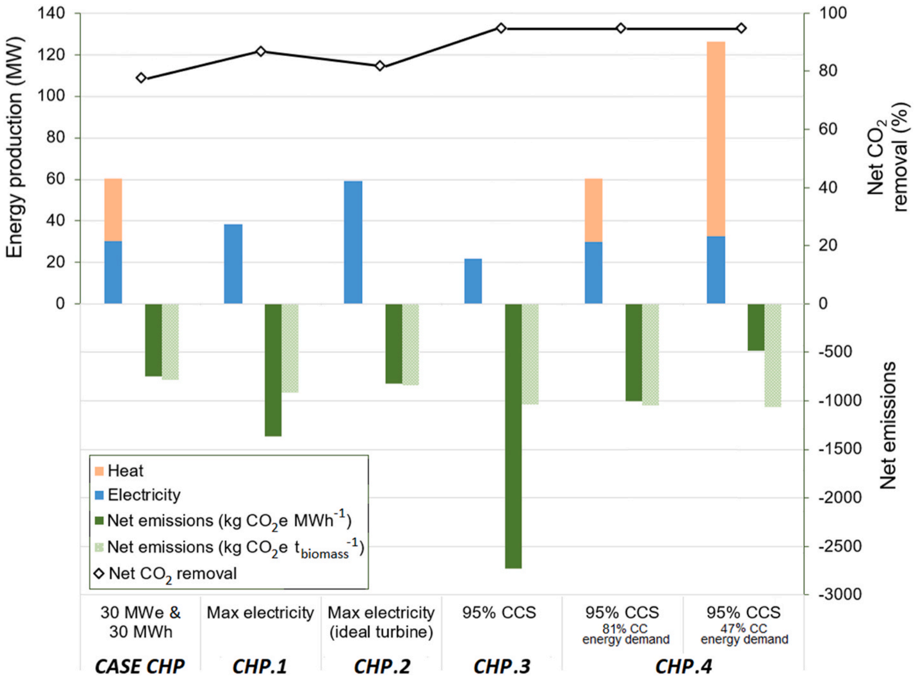

Fig. 8. Alternative operation analysis for the CHP process with post-combustion carbon capture fuelled with wheat straw (Case CHP). The score of three key parameters, namely energy output, carbon capture yield, and net emissions delivered, are represented for each operation mode evaluated. Two metrics were selected to plot net emissions, i.e. the CO_2 equivalents per unit of energy produced and CO_2 equivalents per tonne of biomass used.

e. kg CO_2e MWh^{-1}. Nevertheless, this metric does not indicate how efficient the use of biomass is when biomass availability is a limiting factor for BECCS systems to produce the energy. All the six alternative operation scenarios consumed the same amount of biomass. In order to have a better understanding of how efficiently the biomass was utilised to supply energy while creating negative emissions, the mass-specific emissions factor, i.e. kg CO_2e $t_{biomass}$$^{-1}$ was plotted in Fig. 8. The CDR scores of the investigated scenarios were closer. Scenario CHP.3 scored the highest net negative emissions per MWh produced by the system. On a mass basis, the CDR potential of this scenario (−1027 CO_2e $t_{biomass}$$^{-1}$) was superior to the lowest score reported (773 CO2e tbiomass-1) associated with the baseline Case CHP. However, that difference (33% higher) is not as impressive as the difference for the energy-specific score (266% higher). Therefore, it can be concluded that the excellent

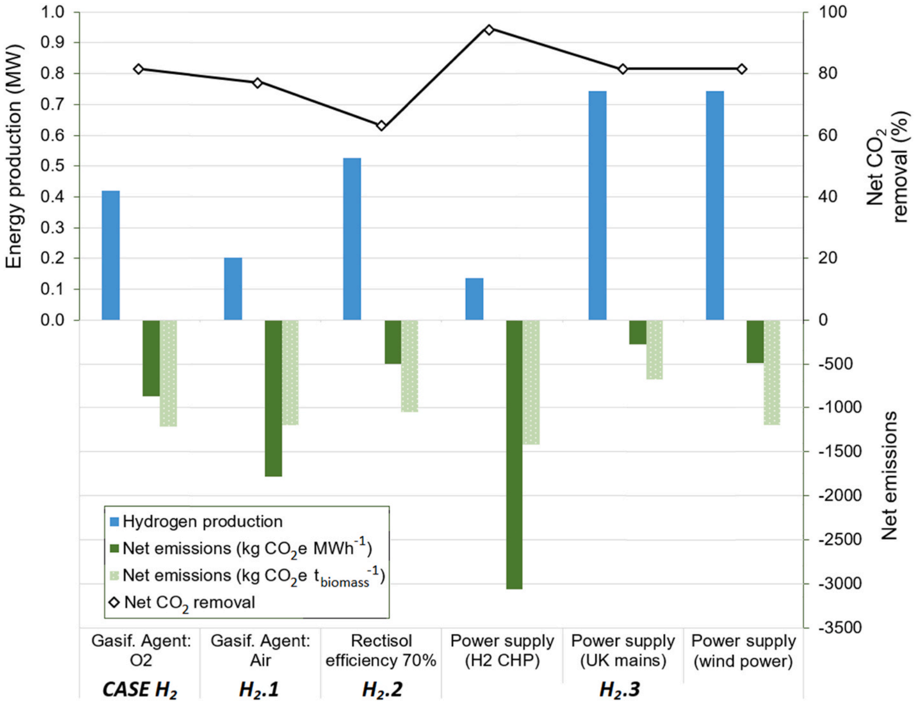

Fig. 9. Alternative operation analysis for the gasification process with pre-combustion carbon capture fuelled with waste wood (Case H_2). The score of three key parameters, namely energy output, carbon capture yield, and net emissions delivered, are represented for each operation mode evaluated. Two metrics were selected to plot net emissions, i.e. the CO_2 equivalents per unit of energy produce and CO_2 equivalents per tonne of biomass used.

energy-specific score resulted mainly from the much lower energy delivered by the system while using the same amount of biomass. In a hypothetical scenario where sustainable biomass resources were unlimited, the preference for Scenario CHP.3 would be straightforward. Conversely, trade-offs between energy production and negative emissions must be accounted for in a real scenario with high competition for the biomass feedstock supply. Using the same among of wheat straw to produce only electricity while using all the heat generated in the CO_2 capture unit (Scenario CHP.1) caused a percentage increase in both power production (28%) and net-negative emissions (-835 CO_2e $t_{biomass}{}^{-1}$, i.e. +17%) when compared to Case CHP.

Since the CDR score on a mass-specific basis was not sensitive to process operation, increasing efficiencies, i.e. by choosing a more efficient turbine (Scenario CHP.2) or by optimising the energy efficiency of the amine scrubbing system (Scenarios CHP.4), would increase the energy production while delivering similar net-negative emissions using the same amount of sustainable biomass.

4.3. Case H_2 alternative operation scenarios

Changes in the operation mode for Case H_2 also influenced both performance parameters and CDR results. Fig. 9 illustrates the results from the Case Study B assessment, comparing energy production, net CO_2 removal ratio and net emissions of the different scenarios.

Scenario H_2.1 used air instead of oxygen as a gasification agent, resulting in lower biomass-to-hydrogen efficiency. When using air, nitrogen enters the system along with the oxygen required for gasification. This increases the producer gas flow compared to the baseline operation using oxygen, and a more significant fraction of the producer gas needs to be burnt for internal heat supply. More Rectisol is required to maintain the CO_2 capture yield, which means a higher fraction of H_2 is used for the internal power supply. As a result, hydrogen production dropped by 52%, and a lower CO_2 capture yield was reported. Net-negative emissions per unit of energy doubled due to an increased requirement for biomass.

Scenario H_2.2 quantified the existing tradeoffs between energy vector production rate and CO_2 capture rate at the Rectisol unit. Reducing Rectisol yield from 98% to 70% resulted in a 25% increase in hydrogen production rate. A smaller fraction of producer gas was burnt for internal heat supply as the solvent flow was reduced. While the internal power demand was reduced due to lower CO_2 compression and solvent cooling requirements, more energy was needed for cooling the higher syngas flow. In addition, a more complex membrane system was needed to purify the H_2 stream with higher CO_2 concentration [114]. This resulted in higher CO_2 emissions from the waste gas leaving the membrane. Thus, despite higher H_2 production, Scenario H_2.2 reported lower net-negative emissions per MWh.

Scenarios H_2.3 evaluate the impact of different electricity sources on internal processes. Using H_2 with fuel cell purity in a combustion CHP system delivered the lowest hydrogen production [115] and CO_2 emissions. Only 33% of the baseline H_2 output was achieved, while net-negative emissions were 255% higher. Assuming external power supply from the UK grid maximised the H_2 output showing a percentage increase of 77% with respect to Case H_2. However, while the CO_2 capture rate was high, the CDR benefits from the BECCS system were offset by the emissions related to grid electricity, resulting in the lowest net-negative potential of the compared options. This would be expected to change with the decarbonisation of UK electricity. The power-to-gas operation, considering 100% renewable electricity from external sources, would achieve the maximum H_2 production rate while incorporating energy storage purposes. However, this scenario would still have a lower CDR potential score than the baseline as less biomass and therefore less carbon is entering the system to produce additional hydrogen to support internal processes.

As in the CHP scenarios, further conclusions can be drawn when computing the CDR score on a mass-specific basis. The differences in the net-negative emissions delivered per tonne of biomass fed to the alternative operation scenarios were buffered (see Fig. 9). Using oxygen as a gasification agent (Case H_2) resulted in superior hydrogen production than using air (Scenario H_2.1), while both scenarios delivered similar net-negative emissions (-1200 and -1197 CO_2e $t_{biomass}{}^{-1}$, respectively). The extra emissions from the air separation unit to produce oxygen were comparable to the loss in process efficiency from using air. When the CO_2 capture yield was reduced to produce more hydrogen (Scenario H_2.2), the CDR potential per tonne of biomass consumed was reduced by 14% (-1038 CO_2e $t_{biomass}{}^{-1}$) compared to the benchmark hydrogen case study. This is a lower percentage variation to the increase in hydrogen production rate (25%), and including an H_2 CHP unit for internal heat supply increases the process net-negative emissions by 17% (-1405 CO_2e $t_{biomass}{}^{-1}$). Whenever feedstock availability is limited, the high impact on hydrogen production makes Scenario H_2.3 (i) discouraging. On the other hand, increasing hydrogen production rate by powering the system using the mains (Scenario H_2.3 (ii)) resulted in the highest impact on net-negative emissions, showing a 44% reduction (-671 CO_2e $t_{biomass}{}^{-1}$) due to the environmental impact associated with power production in the UK. If wind power supply were possible for a power-to-gas operation, the maximum H_2 production could be achieved while simultaneously delivering similar net-negative emissions (-1185 CO_2e $t_{biomass}{}^{-1}$) than the benchmark case study with the same amount of biomass used.

4.4. Role of BECCS in meeting the UK's net-zero targets

The results of the CDR potential were used to estimate the number of facilities required to reach the UK's CDR target of 20 Mt CO_2 p.a., which is the lowest benchmark BECCS is required to deliver the UK's net-zero targets (see Table 8).

For Case CHP, 64 modular CHP plants would be required to achieve that goal. The CHP facilities would have a maximum joint capacity of 1.9 GWe and 1.9 GWth to produce 13.5 TWh of electricity annually and 13.5 TWh of heat while requiring 26.0 Mt of wheat straw p.a. That electricity supply would cover 4% of the total electricity demand in the UK (346 TWh in 2019) [116]. In addition, the heat generated would supply 2% of the UK annual heat demand (726 TWh [117]) and support the current heat networks capacity (14.5 TWh in 2019 [116]).

Considering the results from the evaluation of the alternative technical configurations for each process that involve dissimilar net negative emissions scores, the number of facilities to achieve 20 Mt CO_2 p.a. and related energy output will change as presented in Table 8. Scenario CHP.1 would require 55 facilities with a combined capacity of 2.1 GWe producing 14.9 TWh p.a. Scenario CHP.2 would require 59 facilities (3.5 GWe) producing 24.5 TWh p.a. of electricity. For Scenario CHP.3, 48 facilities (1.1 GWe) would be required, producing 7.4 TWh p.a. electricity. For Scenarios CHP.4, (i) 48 facilities (1.4 GWe and 1.4 GWth) would be needed producing 10.1 TWh p.a. electricity, and 10.2 TWh p.a. heat or (ii) 47 facilities (1.6 GWe and 4.5 GWth) would produce 10.7 TWh p.a. electricity and 31.3 TWh p.a. heat.

For Case H_2, 7903 facilities would be needed to remove 20 Mt CO_2 p.a. They would have a collective hydrogen production capacity of 3.3 GW (23.3 TWh produced p.a.) and consume 16.6 Mt of wood pellets annually. The facilities would supply two-thirds of the UK's low-carbon hydrogen production goal (5 GW) for 2030 [20]. As for Case CHP, the different scenarios for Case H_2 demonstrated the variability in CDR and H_2/energy supply potential. Scenario H_2.1 would require 7946 facilities (1.6 GW of net-capacity) with a combined production of 11.3 TWh p.a. For Scenario H_2.2, 11,067 facilities would be needed to reach the CDR minimum target, providing a net-capacity of 5.8 GW and producing 40.7 TWh p.a. Scenario H_2.3, using an H_2 CHP unit for internal power supply, demonstrated the highest CDR potential, requiring 6771 facilities, due to the much higher biomass demand. This Scenario also has the lowest H_2/energy output of 0.9 GW, with 6.6 TWh generated annually. Using grid electricity in Scenario H_2.3 almost doubled the number of

Table 8

Annual biomass requirements and energy output for the two bioenergy production systems, including their operational alternatives to reach the lowest UK's CDR target, i.e. 20 Mt CO_2 p.a., set for BECCS. A colour scale has been used to sort the different scenarios from most preferrable (green) to least preferrable (red) for a specific parameter.

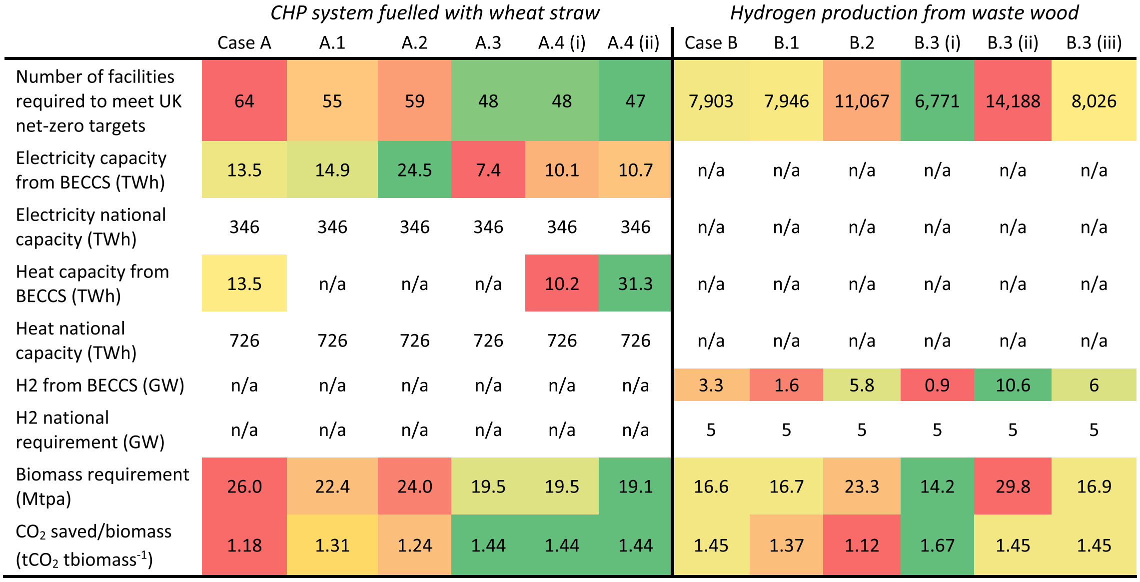

	CHP system fuelled with wheat straw						Hydrogen production from waste wood					
	Case A	A.1	A.2	A.3	A.4 (i)	A.4 (ii)	Case B	B.1	B.2	B.3 (i)	B.3 (ii)	B.3 (iii)
Number of facilities required to meet UK net-zero targets	64	55	59	48	48	47	7,903	7,946	11,067	6,771	14,188	8,026
Electricity capacity from BECCS (TWh)	13.5	14.9	24.5	7.4	10.1	10.7	n/a	n/a	n/a	n/a	n/a	n/a
Electricity national capacity (TWh)	346	346	346	346	346	346	n/a	n/a	n/a	n/a	n/a	n/a
Heat capacity from BECCS (TWh)	13.5	n/a	n/a	n/a	10.2	31.3	n/a	n/a	n/a	n/a	n/a	n/a
Heat national capacity (TWh)	726	726	726	726	726	726	n/a	n/a	n/a	n/a	n/a	n/a
H2 from BECCS (GW)	n/a	n/a	n/a	n/a	n/a	n/a	3.3	1.6	5.8	0.9	10.6	6
H2 national requirement (GW)	n/a	n/a	n/a	n/a	n/a	n/a	5	5	5	5	5	5
Biomass requirement (Mtpa)	26.0	22.4	24.0	19.5	19.5	19.1	16.6	16.7	23.3	14.2	29.8	16.9
CO_2 saved/biomass (tCO_2 $tbiomass^{-1}$)	1.18	1.31	1.24	1.44	1.44	1.44	1.45	1.37	1.12	1.67	1.45	1.45

required facilities compared to the baseline with 14,188 facilities offering a capacity of 10.6 GW, to produce 74.0 TWh p.a. This Scenario would also have the highest biomass demand of 29 Mt p.a. Switching to 100% renewable energy for internal energy use would reduce these numbers to 8026 facilities offering a combined net-capacity of 6.0 GW, annually producing 41.8 TWh.

The results from the assessment show the synergies between CDR potential, energy generation and biomass requirements. However, these aspects can change depending on the key system drivers, with significant implications on supply chain, demand, and investment requirements. Scenario CHP.3, A.4 (i and ii) and B.3 (i) require the lowest number of facilities to deliver 20 Mt CO_2 removal p.a, but their energy output can be lower than the baselines and other operational alternatives as they focus on maximising CDR. Scenario CHP.2, B.2 and B.3 (ii) require a much larger number of facilities, consequently delivering a higher energy output, but also requiring large amounts of biomass. While a low biomass-to energy efficiency increases the CDR potential, policies and business models need to consider such system dynamics to ensure that the strong focus on CDR does not undermine other environmental, economic and social sustainability aspects.

However, reaching the 20 Mt CO_2 removal p.a target seems challenging when considering only nationally sourced biomass. Currently, a wheat straw surplus of 1.7 Mt p.a. and a waste wood surplus of 3.3 Mt p.a. (assuming all the spare waste wood was pelletised and had an average bulk density of 650 kg/m^3 on a dry basis, as considered in the LCA) would be available in the UK to produce bioenergy. Considering that all available resources were used for facilities as described in Cases A and B, only 4 CHP facilities could be operated removing 1.3 Mt CO_2 p.a., and 1247 wood pellet gasification facilities removing 3.2 Mt CO_2 p.a. In terms of energy supply, converting the available wheat straw using Case CHP technology would supply less than 1% of the UK electricity and heat demands, while utilising all the UK's waste wood surplus in Case H_2 facilities could provide a 10% of the UK's low-carbon hydrogen production goal. The joint CDR capacity for both systems accounted for about 23% of the UK's CDR target from BECCS.

Dedicating more land, considering additional feedstocks or importing biomass would be therefore required for both technologies to reach the 20 Mt CO_2 p.a. objective, which would likely change the associated lifecycle and net emissions. An estimate of the land requirements for feedstock supply in the UK, to achieve this target, can be computed from the results of the model. When assuming an average wheat straw yield of 3.90 $t_{ws}ha^{-1}$ [51], reaching BECCS minimum CDR objective would require between 5 and 7 Mha of arable land growing wheat and dedicating the coproduced straw entirely to supply BECCS facilities. When gasification of forest residue to produce hydrogen fuel is considered, and an average forest residue yield of 15.8 $t_{fr}ha^{-1}$ is assumed [97], between 0.9 and 1.5 Mha of woodland entirely dedicated to supply these type of facilities would be needed to remove 20 Mt CO_2 p.a. Variation within the reported range for land requirements correspond to different ways to operate the energy process. Lower land requirements would be achieved when the processes operate maximising the carbon capture ratio, while the greatest land requirements correspond to the same processes aimed at optimising the energy production. Land requirements are therefore really high, considering that in the UK, approximately 4.2 Mha are used for arable crops [118] and the total woodland is estimated as 3.2 Mha [63].

4.5. Decentralised BECCS deployment to meet CDR expectations

These studies showed that BECCS is a feasible option for CDR while producing a range of low-carbon energy vectors, i.e. electricity, heat or hydrogen. All case studies and scenarios evaluated gave net-negative emissions. Therefore, the CDR potential is true, but BECCS expectations are very optimistic as our assessment highlighted a big gap between present deployment and CDR requirements. Low emission scenarios of the IPCC consider large-scale deployment of BECCS by 2050; however, the increasing climate emergency requires immediate action [119]. The assessment showed that decentralised BECCS deployment comprises commercially proven technologies and could represent a starting point to deliver negative emissions in the very short term.

Previous studies identified the competition for investment with cheap renewable energies –e.g. solar and wind– as one of the major barriers for BECCS implementation [49,120]. The modular approach could help overcome that barrier as it commonly involves smaller unit costs, quicker build schedules, and less risk to investors. Therefore, experience demonstrating BECCS technology performance would be generated, which could help attract investment to establish large-scale BECCS deployment that could help reach the CDR targets in the medium-to long term. However, time is also needed to establish CO_2 transport and storage infrastructures at the required scale. While our assessment considered CO_2 storage for simplistic comparison between operational variations, a decentralised approach, based on the results obtained from this work, can produce CO_2 of high purity that could be stored and used for other industrial purposes and generate extra revenues. Depending on the final destination of the $CO_{2,}$ this could potentially create additional CDR benefits.

The biomass-to-energy conversion processes have low efficiency. Results from this study have shown that drops in efficiency led to higher CDR potential outcomes. However, that is not necessarily positive since sustainable biomass resources are limited and risk sustainability implications for feedstock sourcing [121,122]. The previous section concluded that biomass imports would be required to reach the UK's CDR targets set for BECCS. Therefore, multiple BECCS technologies and pathways should be considered to try utilising all the different sustainable biomass feedstock suitable for generating different energy vectors and products. A decentralised vision for BECCS deployment could ease accessibility and enable utilisation of regionally sourced biomass and residues for energy production, primarily aiming at local provision, while also offering improved functionality and flexibility on the energy production pathway for the large-scale counterparts.

5. Conclusions

BECCS is expected to support making net-zero emissions a reality in the UK by 2050, however currently no BECCS plant is operating. Since technological barriers for BECCS deployment are minimal (this study has considered only commercially demonstrated technologies) and sustainable biomass is available, an imminent generation of bioenergy and negative emissions could be achieved. To perform an exhaustive LCA evaluating the carbon intensity of each stage in the whole supply chain is fundamental to determine their actual CDR, and therefore estimating a more accurate contribution of BECCS to a net-zero scenario.

A decentralised BECCS deployment is suggested and investigated. This vision can bring benefits such as reducing the risk for investors, providing industrial learning, and enhanced resilience to market conditions. Sustainable biomass resources are limited. This study estimated that utilising all wheat straw and waste wood available in the UK could achieve 23% of the lowest CDR target (20 Mt p.a.) set for BECCS. A decentralise deployment could enable the accessibility of a variety of additional regional biomass resources. Improved flexibility (the small-scale process can involve the most suitable bioenergy conversion technology for each feedstock) and functionality (the convenient energy vector can be locally supplied) could be achieved. Although CO_2 geological storage was the first option considered here, the study demonstrated that the highly pure CO_2 recovered (>99.0%) is suitable for entering the utilisation market so that the BECCS system could be economically supported and circular economy is endorsed.

The study also concluded that the net-negative potential of investigated BECCS system varies depending on the key performance parameters, i.e. the operating strategy followed. Flexible energy systems might lead to decisions maximising energy production. On the other hand, support for hydrogen production could also disincentivise delivering the highest net-negative emissions possible.

Possible trade-offs between bioenergy production and net-negative emissions generation have been identified and quantified. The energy efficiency of the two investigated systems (CHP and H_2 from gasification) ranged between 10 and 48% depending on the selected operational choice. The energy penalty caused by the carbon capture system (the reported efficiency of similar systems with no CDR unit are 20–30% higher [123,124]) could compromise the economic performance of bioenergy production. Policy frameworks can be a significant driver for the choice of technology and market strategy of BECCS. For example, carbon tax or the creation of markets for emission offsets [125] could shape trajectories for high CDR but low-energy operations. However, a higher CDR score on an energy-specific basis, a frequent metric used to compare alternative energy sources, does not imply that operation mode is preferable. Since biomass availability is limited, biomass-to-energy efficiency must also be considered. Therefore, CDR score on a mass-specific basis is suggested when bioenergy processes are investigated to help identify the most beneficial scenario representing at once the three key parameters: energy output, CDR potential and biomass usage.

Acknowledgement

This work was conduted as part of 'Feasibility of Afforestation and Biomass Energy with Carbon Capture and Storage for Greenhouse Gas Removal' (FAB-GGR) project, funded by the Natural Environment Research Council (NERC) (Grant number: NE/P019722/2) and was supported by the EPSRC/BBSRC Supergen Bioenergy Hub (Grant number: EP/S000771/1). All relevant data is available as supplementary information linked to this article.

Appendix A. Supplementary data

Supplementary data to this article can be found online at https://doi.org/10.1016/j.biombioe.2022.106406.

References

[1] H. Ritchie, M. Roser, CO₂ and Greenhouse Gas Emissions, 2020. https://ourworldindata.org/co2-and-other-greenhouse-gas-emissions#citation. (Accessed 11 May 2021).
[2] CCC, Reducing UK Emissions: Progress Report to Parliament, Committe on Climate Change, 2020.
[3] UNFCCC, Adoption of the Paris Agreement - FCCC/CP/2015/L.9/Rev 1, 2015.
[4] K. Anderson, G. Peters, The trouble with negative emissions, Science 354 (6309) (2016) 182.
[5] W. Burns, S. Nicholson, Bioenergy and carbon capture with storage (BECCS): the prospects and challenges of an emerging climate policy response, J. Environ. Stud. Sci. 7 (4) (2017) 527–534.
[6] C. Azar, D.J.A. Johansson, N. Mattsson, Meeting global temperature targets—the role of bioenergy with carbon capture and storage, Environ. Res. Lett. 8 (3) (2013), 034004.
[7] J.A. Raven, A.J. Karley, Carbon sequestration: photosynthesis and subsequent processes, Curr. Biol. 16 (5) (2006) R165–R167.
[8] J. Zhang, X. Zhang, 15 - the thermochemical conversion of biomass into biofuels, in: D. Verma, E. Fortunati, S. Jain, X. Zhang (Eds.), Biomass, Biopolymer-Based Materials, and Bioenergy, Woodhead Publishing2019, pp. 327-368.
[9] J. Gibbins, H. Chalmers, Carbon capture and storage, Energy Pol. 36 (12) (2008) 4317–4322.
[10] Y. Wang, L. Zhao, A. Otto, M. Robinius, D. Stolten, A review of post-combustion CO2 capture technologies from coal-fired power plants, Energy Proc. 114 (2017) 650–665.
[11] A. Raza, R. Gholami, R. Rezaee, V. Rasouli, M. Rabiei, Significant aspects of carbon capture and storage – a review, Petroleum 5 (4) (2019) 335–340.
[12] C. Azar, K. Lindgren, E. Larson, K. Möllersten, Carbon capture and storage from fossil fuels and biomass – costs and potential role in stabilizing the atmosphere, Climatic Change 74 (1) (2006) 47–79.
[13] V. Barlet-Gouédard, G. Rimmelé, B. Goffé, O.J.O. Porcherie, G. Science, T.-R. IFP, Well technologies for CO2, Geological Storage: CO2-Resistant Cement 62 (3) (2007) 325–334.
[14] C. Escamilla-Alvarado, J.A. Pérez-Pimienta, T. Ponce-Noyola, H.M. Poggi-Varaldo, An overview of the enzyme potential in bioenergy-producing biorefineries, J. Chem. Technol. Biotechnol. 92 (5) (2017) 906–924.
[15] C.L. Williams, A. Dahiya, P. Porter, in: A. Dahiya (Ed.), Chapter 1 - Introduction to Bioenergy, Bioenergy, Academic Press, Boston, 2015, pp. 5–36.
[16] N.E. Vaughan, C. Gough, S. Mander, E.W. Littleton, A. Welfle, D.E.H.J. Gernaat, D.P. van Vuuren, Evaluating the use of biomass energy with carbon capture and storage in low emission scenarios, Environ. Res. Lett. 13 (4) (2018), 044014.
[17] N. Bauer, K. Calvin, J. Emmerling, O. Fricko, S. Fujimori, J. Hilaire, J. Eom, V. Krey, E. Kriegler, I. Mouratiadou, H. Sytze de Boer, M. van den Berg, S. Carrara, V. Daioglou, L. Drouet, J.E. Edmonds, D. Gernaat, P. Havlik, N. Johnson, D. Klein, P. Kyle, G. Marangoni, T. Masui, R.C. Pietzcker, M. Strubegger, M. Wise, K. Riahi, D.P. van Vuuren, Shared socio-economic pathways of the energy sector – quantifying the narratives, Global Environ. Change 42 (2017) 316–330.

[18] V. Masson-Delmotte, P. Zhai, H.-O. Pörtner, D. Roberts, J. Skea, P.R. Shukla, A. Pirani, W. Moufouma-Okia, C. Péan, R. Pidcock, S. Connors, J.B.R. Matthews, Y. Chen, X. Zhou, M.I. Gomis, E. Lonnoy, T. Maycock, M. Tignor, T. Waterfield, Global Warming of 1.5°C. An IPCC Special Report on the Impacts of Global Warming of 1.5°C above Pre-industrial Levels and Related Global Greenhouse Gas Emission Pathways, in the Context of Strengthening the Global Response to the Threat of Climate Change, Sustainable Development, and Efforts to Eradicate Poverty, Intergovernmental Panel on Climate Change (IPCC), 2018.

[19] A. Wiltshire, T. Davies-Barnard, C. Jones, Planetary Limits to BECCS Negative Emissions, Department of Energy and Climate Change (DECC), 2015.

[20] U. Government, The Energy White Paper - Powering Our Net Zero Future, 2020.

[21] P. Smith, R.S. Haszeldine, S.M. Smith, Preliminary assessment of the potential for, and limitations to, terrestrial negative emission technologies in the UK, Environ. Sci.: Processes & Impacts 18 (11) (2016) 1400–1405.

[22] T.R. Society, Greenhouse Gas Removal, 2018.

[23] M. Fridahl, M. Lehtveer, Bioenergy with carbon capture and storage (BECCS): global potential, investment preferences, and deployment barriers, Energy Res. Social Sci. 42 (2018) 155–165.

[24] S.V. Hanssen, V. Daioglou, Z.J.N. Steinmann, J.C. Doelman, D.P. Van Vuuren, M. A.J. Huijbregts, The climate change mitigation potential of bioenergy with carbon capture and storage, Nat. Clim. Change 10 (2020) 1023–1029, https://doi.org/10.1038/s41558-020-0885-y.

[25] N.E. Vaughan, C. Gough, Expert assessment concludes negative emissions scenarios may not deliver, Environ. Res. Lett. 11 (9) (2016), 095003.

[26] C. Consloli, Bioenergy and Carbon Capture and Storage - 2019 Perspective, Global CCS Institute, 2019.

[27] Toshiba, Toshiba Starts Operation of Large-Scale Carbon Capture Facility, 2020. https://www.toshiba-energy.com/en/info/info2020_1031.htm. (Accessed 12 May 2021).

[28] Drax, Our BECCS Projects and Partnerships, 2020. https://www.drax.com/about-us/our-projects/bioenergy-carbon-capture-use-and-storage-beccs/. (Accessed 12 May 2021).

[29] R.E. Environment, Analysing the Potential of Bioenergy with Carbon Capture in the UK to, 2020, p. 2050.

[30] T. Seitarides, C. Athanasiou, A. Zabaniotou, Modular biomass gasification-based solid oxide fuel cells (SOFC) for sustainable development, Renew. Sustain. Energy Rev. 12 (5) (2008) 1251–1276.

[31] L. Dong, H. Liu, S. Riffat, Development of small-scale and micro-scale biomass-fuelled CHP systems – a literature review, Appl. Therm. Eng. 29 (11) (2009) 2119–2126.

[32] M. Röder, C. Jamieson, P. Thornley, (Stop) burning for biogas. Enabling positive sustainability trade-offs with business models for biogas from rice straw, Biomass Bioenergy 138 (2020) 105598.

[33] B. Mignacca, G. Locatelli, Economics and finance of Small Modular Reactors: a systematic review and research agenda, Renew. Sustain. Energy Rev. 118 (2020) 109519.

[34] M. Aresta, Carbon dioxide utilization: the way to the circular economy, Greenhouse Gases: Sci. Technol. 9 (4) (2019) 610–612.

[35] A.A. Al-Yaeeshi, R. Govindan, T. Al-Ansari, Techno-economic-based dynamic network design for optimum large-scale carbon dioxide utilisation in process industries, J. Clean. Prod. 275 (2020) 122974.

[36] H. Zhang, L. Wang, J. Van herle, F. Maréchal, U. Desideri, Techno-Economic Optimization of CO2-to-Methanol with Solid-Oxide Electrolyzer 12, 2019, p. 3742, 19.

[37] M. Aresta, Carbon Dioxide as Chemical Feedstock, Wiley-VCH2010.

[38] E. Alper, O. Yuksel Orhan, CO2 utilization: developments in conversion processes, Petroleum 3 (1) (2017) 109–126.

[39] F.G. Acién Fernández, C.V. González-López, J.M. Fernández Sevilla, E. Molina Grima, Conversion of CO2 into biomass by microalgae: how realistic a contribution may it be to significant CO2 removal? Appl. Microbiol. Biotechnol. 96 (3) (2012) 577–586.

[40] D. Ravikumar, D. Zhang, G. Keoleian, S. Miller, V. Sick, V. Li, Carbon dioxide utilization in concrete curing or mixing might not produce a net climate benefit, Nat. Commun. 12 (1) (2021) 855.

[41] C.-H. Huang, C.-S. Tan, A review: CO2 utilization, Aerosol Air Qual. Res. 14 (2) (2014) 480–499.

[42] M. North, Chapter 1 - what is CO2? Thermodynamics, basic reactions and physical chemistry, in: P. Styring, E.A. Quadrelli, K. Armstrong (Eds.), Carbon Dioxide Utilisation, Elsevier, Amsterdam, 2015, pp. 3–17.

[43] M. Bui, C.S. Adjiman, A. Bardow, E.J. Anthony, A. Boston, S. Brown, P.S. Fennell, S. Fuss, A. Galindo, L.A. Hackett, J.P. Hallett, H.J. Herzog, G. Jackson, J. Kemper, S. Krevor, G.C. Maitland, M. Matuszewski, I.S. Metcalfe, C. Petit, G. Puxty, J. Reimer, D.M. Reiner, E.S. Rubin, S.A. Scott, N. Shah, B. Smit, J.P.M. Trusler, P. Webley, J. Wilcox, N. Mac Dowell, Carbon capture and storage (CCS): the way forward, Energy Environ. Sci. 11 (5) (2018) 1062–1176.

[44] BEIS, Combined Heat and Power: the Route to 2050, Department for Business, Energy & Industrial Strategy, UK Government, 2020.

[45] K. Sipilä, 3 - cogeneration, biomass, waste to energy and industrial waste heat for district heating, in: R. Wiltshire (Ed.), Advanced District Heating and Cooling (DHC) Systems, Woodhead Publishing, Oxford, 2016, pp. 45–73.

[46] M. Börjesson, E.O. Ahlgren, 5.07 - biomass CHP energy systems: a critical assessment, in: A. Sayigh (Ed.), Comprehensive Renewable Energy, Elsevier, Oxford, 2012, pp. 87–97.

[47] R. Padinger, S. Aigenbauer, C. Schmidl, Best Practise Report on Decentralized Biomass Fired CHP Plants and Status of Biomass Fired Small- and Micro Scale CHP Technologies, IEA Bioenergy, 2019.

[48] C. Robledo-Abad, H.-J. Althaus, G. Berndes, S. Bolwig, E. Corbera, F. Creutzig, J. Garcia-Ulloa, A. Geddes, J.S. Gregg, H. Haberl, S. Hanger, R.J. Harper, C. Hunsberger, R.K. Larsen, C. Lauk, S. Leitner, J. Lilliestam, H. Lotze-Campen, B. Muys, M. Nordborg, M. Ölund, B. Orlowsky, A. Popp, J. Portugal-Pereira, J. Reinhard, L. Scheiffle, P. Smith, Bioenergy production and sustainable development: science base for policymaking remains limited, 3 9, 2017, pp. 541–556.

[49] N. Pour, Chapter 13 - economics and policy of bioenergy with carbon capture and storage, in: J.C. Magalhães Pires, A.L.D. Cunha Gonçalves (Eds.), Bioenergy with Carbon Capture and Storage, Academic Press2019, pp. 257-271.

[50] G. Mattias, T. Elena, C. Giuseppe, F.E. Anna, Modeling the ecosystem service of agricultural residues provision for bioenergy production: a potential application in the Emilia-Romagna region (Italy), Ecol. Model. 451 (2021) 109571.

[51] DEFRA, Crops Grown for Bioenergy in the UK: 2018, Department for Environment, Food & Rural Affairs, 2019.

[52] A. Padurean, C.-C. Cormos, P.-S. Agachi, Pre-combustion carbon dioxide capture by gas–liquid absorption for Integrated Gasification Combined Cycle power plants, Int. J. Greenh. Gas Control 7 (2012) 1–11.

[53] A.L. Kohl, R.B. Nielsen, Chapter 2 - alkanolamines for hydrogen sulfide and carbon dioxide removal, in: A.L. Kohl, R.B. Nielsen (Eds.), Gas Purification, fifth ed., Gulf Professional Publishing, Houston, 1997, pp. 40–186.

[54] U.K. Government, Industrial Decarbonisation Strategy, 2021 https://assets.publishing.service.gov.uk/government/uploads/system/uploads/attachment_data/file/970229/Industrial_Decarbonisation_Strategy_March_2021.pdf.

[55] DfT, Decarbonising Transport, UK Government - Department for Transport, 2020.

[56] U.K. Government, The Ten Point Plan for a Green Industrial Revolution, 2020. https://assets.publishing.service.gov.uk/government/uploads/system/uploads/attachment_data/file/936567/10_POINT_PLAN_BOOKLET.pdf.

[57] K. Mazloomi, C. Gomes, Hydrogen as an energy carrier: prospects and challenges, Renew. Sustain. Energy Rev. 16 (5) (2012) 3024–3033.

[58] M. Yue, H. Lambert, E. Pahon, R. Roche, S. Jemei, D. Hissel, Hydrogen energy systems: a critical review of technologies, applications, trends and challenges, Renew. Sustain. Energy Rev. 146 (2021) 111180.

[59] L. Cao, I.K.M. Yu, X. Xiong, D.C.W. Tsang, S. Zhang, J.H. Clark, C. Hu, Y.H. Ng, J. Shang, Y.S. Ok, Biorenewable hydrogen production through biomass gasification: a review and future prospects, Environ. Res. 186 (2020) 109547.

[60] S. Hinson, A. Adcock, UK Hydrogen Economy, The House of Commons Library, 2020.

[61] Y.H. Chan, K.W. Cheah, B.S. How, A.C.M. Loy, M. Shahbaz, H.K.G. Singh, N.a. R. Yusuf, A.F.A. Shuhaili, S. Yusup, W.A.W.A.K. Ghani, J. Rambli, Y. Kansha, H. L. Lam, B.H. Hong, S.L. Ngan, An overview of biomass thermochemical conversion technologies in Malaysia, Sci. Total Environ. 680 (2019) 105–123.

[62] J.M. Bermudez, B. Fidalgo, 15 - production of bio-syngas and bio-hydrogen via gasification, in: R. Luque, C.S.K. Lin, K. Wilson, J. Clark (Eds.), Handbook of Biofuels Production (second ed.), Woodhead Publishing2016, pp. 431-494.

[63] R. Stagg, S. Ward, Forestry Statistics 2020, Forest Research - UK Government, 2020.

[64] G. Charis, G. Danha, E. Muzenda, A review of timber waste utilization: challenges and opportunities in Zimbabwe, Procedia Manuf. 35 (2019) 419–429.

[65] A. Paethanom, S. Nakahara, M. Kobayashi, P. Prawisudha, K. Yoshikawa, Performance of tar removal by absorption and adsorption for biomass gasification, Fuel Process. Technol. 104 (2012) 144–154.

[66] S.I. Meramo-Hurtado, P. Puello, A. Cabarcas, Process analysis of hydrogen production via biomass gasification under computer-aided safety and environmental assessments, ACS Omega 5 (31) (2020) 19667–19681.

[67] W.L. Theo, J.S. Lim, H. Hashim, A.A. Mustaffa, W.S. Ho, Review of pre-combustion capture and ionic liquid in carbon capture and storage, Appl. Energy 183 (2016) 1633–1663.

[68] S. Yang, Y. Qian, S. Yang, Development of a full CO2 capture process based on the Rectisol wash technology, Ind. Eng. Chem. Res. 55 (21) (2016) 6186–6193.

[69] ISO, Hydrogen Fuel Quality - Product Specification, 2019. ISO 14687:2019. https://www.iso.org/standard/69539.html. (Accessed 19 May 2021).

[70] G.W. Huber, S. Iborra, A. Corma, Synthesis of transportation fuels from biomass: chemistry, catalysts, and engineering, Chem. Rev. 106 (9) (2006) 4044–4098.

[71] S. Karellas, Hydrogen production from biomass gasification, in: Z. Fang, J.R. L. Smith, X. Qi (Eds.), Production of Hydrogen from Renewable Resources, Springer Netherlands, Dordrecht, 2015, pp. 97–117.

[72] M. Lototskyy, I. Tolj, Y. Klochko, M.W. Davids, D. Swanepoel, V. Linkov, Metal hydride hydrogen storage tank for fuel cell utility vehicles, Int. J. Hydrogen Energy 45 (14) (2020) 7958–7967.

[73] Q. Ma, L. Han, G. Huang, Evaluation of different water-washing treatments effects on wheat straw combustion properties, Bioresour. Technol. 245 (2017) 1075–1083.

[74] R. Kc, I. Babu, S. Alatalo, J. Föhr, T. Ranta, I. Tiihonen, Hydrothermal carbonization of deciduous biomass (Alnus incana) and pelletization prospects, J. Sustain. Bioenergy Syst. 7 (3) (2017) 10.

[75] O. Emenike, S. Michailos, K.N. Finney, K.J. Hughes, D. Ingham, M. Pourkashanian, Initial techno-economic screening of BECCS technologies in power generation for a range of biomass feedstock, Sustain. Energy Technol. Assessments 40 (2020) 100743.

[76] A. Milićević, S. Belošević, N. Crnomarković, I. Tomanović, D. Tucaković, Mathematical modelling and optimisation of lignite and wheat straw co-combustion in 350 MWe boiler furnace, Appl. Energy 260 (2020) 114206.

[77] M.P. González-Vázquez, F. Rubiera, C. Pevida, D.T. Pio, L.A.C. Tarelho, Thermodynamic analysis of biomass gasification using aspen Plus: comparison of stoichiometric and non-stoichiometric models, Energies 14 (1) (2021).

[78] M. Martin, Introduction to Software for Chemical Engineers (second ed.), CRC Press2019.

[79] J. Lee, S. Yu, J. Park, H. Jo, J. Park, C. Ryu, Y.-g. Jeong, Reduction of unburned carbon release and NOx emission from a pulverized wood pellet boiler retrofitted for fuel switching from coal, Energies 13 (19) (2020).

[80] P. Kaushal, R. Tyagi, Advanced simulation of biomass gasification in a fluidized bed reactor using ASPEN PLUS, Renew. Energy 101 (2017) 629–636.

[81] Y. Zhang, H. Que, C.-C. Chen, Thermodynamic modeling for CO2 absorption in aqueous MEA solution with electrolyte NRTL model, Fluid Phase Equil. 311 (2011) 67–75.

[82] E. Shayan, V. Zare, I. Mirzaee, Hydrogen production from biomass gasification; a theoretical comparison of using different gasification agents, Energy Convers. Manag. 159 (2018) 30–41.

[83] M.W. Islam, A review of dolomite catalyst for biomass gasification tar removal, Fuel 267 (2020) 117095.

[84] K.D. Panopoulos, L.E. Fryda, J. Karl, S. Poulou, E. Kakaras, High temperature solid oxide fuel cell integrated with novel allothermal biomass gasification: Part I: modelling and feasibility study, J. Power Sources 159 (1) (2006) 570–585.

[85] E. Vlad, C. Bildea, P. Valentin, G. Marton, G. Bozga, Process Design of Biodiesel Production from Rapeseed Oil, 61, Revista de Chimie, 2010.

[86] AspenTech, Aspen Physical Property System - Physical Property Methods, 2013.

[87] R.A. Dagle, A. Karim, G. Li, Y. Su, D.L. King, Chapter 12 - syngas conditioning, in: D. Shekhawat, J.J. Spivey, D.A. Berry (Eds.), Fuel Cells: Technologies for Fuel Processing, Elsevier, Amsterdam, 2011, pp. 361–408.

[88] A. Ouadha, M. En nacer, L. Adjlout, O. Imine, Exergy analysis of a two-stage refrigeration cycle using two natural substitutes of HCFC22, Int. J. Exergy - INT J EXERGY 2 (2005).

[89] I. Dincer, 1.7 energy and exergy efficiencies, in: I. Dincer (Ed.), Comprehensive Energy Systems, Elsevier, Oxford, 2018, pp. 265–339.

[90] S. Hopkins, A. Manheim, K. Randolph, High-Performance Palladium Based Membrane for Hydrogen Separation and Purification, Pall Corporation, 2012.

[91] S. Adhikari, S. Fernando, Hydrogen membrane separation techniques, Ind. Eng. Chem. Res. 45 (3) (2006) 875–881.

[92] A. Kazakov, D. Blinov, I. Romanov, D. Dunikov, V. Borzenko, Metal hydride technologies for renewable energy 114, E3S Web Conference, 2019, 05005.

[93] A.A. Rabienataj Darzi, H. Hassanzadeh Afrouzi, A. Moshfegh, M. Farhadi, Absorption and desorption of hydrogen in long metal hydride tank equipped with phase change material jacket, Int. J. Hydrogen Energy 41 (22) (2016) 9595–9610.

[94] G. Finnveden, J. Potting, Life cycle assessment, in: P. Wexler (Ed.), Encyclopedia of Toxicology, third ed., Academic Press, Oxford, 2014, pp. 74–77.

[95] A.M. Tillman, 4 - methodology for life cycle assessment, in: U. Sonesson, J. Berlin, F. Ziegler (Eds.), Environmental Assessment and Management in the Food Industry, Woodhead Publishing2010, pp. 59-82.

[96] E. Comission, ILCD International Life Cycle Data System, 2010. https://eplca.jrc.ec.europa.eu/ilcd.html.

[97] S. García-Freites, C. Gough, M. Röder, The greenhouse gas removal potential of bioenergy with carbon capture and storage (BECCS) to support the UK's net-zero emission target, Biomass Bioenergy 151 (2021) 106164.

[98] S. Njakou Djomo, O. El Kasmioui, T. De Groote, L.S. Broeckx, M.S. Verlinden, G. Berhongaray, R. Fichot, D. Zona, S.Y. Dillen, J.S. King, I.A. Janssens, R. Ceulemans, Energy and climate benefits of bioelectricity from low-input short rotation woody crops on agricultural land over a two-year rotation, Appl. Energy 111 (2013) 862–870.

[99] F. Cherubini, A.H. Strømman, S. Ulgiati, Influence of allocation methods on the environmental performance of biorefinery products—a case study, Resour. Conserv. Recycl. 55 (11) (2011) 1070–1077.

[100] J. van Bennekom, R.H. Venderbosch, H.J. Heeres, Biomethanol from glycerol, in: Z. Fang (Ed.), Biodiesel - Feedstocks, Production and Applications, IntechOpen2012.

[101] I. Dosa, D. Petrilean, Efficiency assessment of condensing steam turbine, Adv. Environ. Ecosyst. Sustain. Tourism (2013) 203–208.

[102] EPA, Catalog of CHP technologies, U.S, Environment and Protection Agency - Combined Heat and Power Partnership, 2017.

[103] H.P. Mangalapally, H. Hasse, Pilot plant study of post-combustion carbon dioxide capture by reactive absorption: methodology, comparison of different structured packings, and comprehensive results for monoethanolamine, Chem. Eng. Res. Des. 89 (8) (2011) 1216–1228.

[104] M. Fajardy, N. Mac Dowell, Can BECCS deliver sustainable and resource efficient negative emissions? Energy Environ. Sci. 10 (6) (2017) 1389–1426.

[105] M.R.M. Abu-Zahra, L.H.J. Schneiders, J.P.M. Niederer, P.H.M. Feron, G. F. Versteeg, CO2 capture from power plants: Part I. A parametric study of the technical performance based on monoethanolamine, Int. J. Greenh. Gas Control 1 (1) (2007) 37–46.

[106] K.W. Harrison, R. Remick, G.D. Martin, A. Hoskin, Hydrogen Production: Fundamentals and Case Study Summaries, 2010. https://www.nrel.gov/docs/fy10osti/47302.pdf.

[107] P. Millet, 9 - hydrogen production by polymer electrolyte membrane water electrolysis, in: V. Subramani, A. Basile, T.N. Veziroğlu (Eds.), Compendium of Hydrogen Energy, Woodhead Publishing, Oxford, 2015, pp. 255–286.

[108] C. Hepburn, E. Adlen, J. Beddington, E.A. Carter, S. Fuss, N. Mac Dowell, J. C. Minx, P. Smith, C.K. Williams, The technological and economic prospects for CO2 utilization and removal, Nature 575 (7781) (2019) 87–97.

[109] H.-J. Ho, A. Iizuka, E. Shibata, Carbon capture and utilization technology without carbon dioxide purification and pressurization: a review on its necessity and available technologies, Ind. Eng. Chem. Res. 58 (21) (2019) 8941–8954.

[110] H. Eldardiry, E. Habib, Carbon capture and sequestration in power generation: review of impacts and opportunities for water sustainability, Energy, Sustain. Soc. 8 (1) (2018) 6.

[111] S.-Y. Oh, M. Binns, H. Cho, J.-K. Kim, Energy minimization of MEA-based CO2 capture process, Appl. Energy 169 (2016) 353–362.

[112] Q. Yi, Y. Zhao, Y. Huang, G. Wei, Y. Hao, J. Feng, U. Mohamed, M. Pourkashanian, W. Nimmo, W. Li, Life cycle energy-economic-CO2 emissions evaluation of biomass/coal, with and without CO2 capture and storage, in a pulverized fuel combustion power plant in the United Kingdom, Appl. Energy 225 (2018) 258–272.

[113] S. García-Freites, C. Gough, M. Röder, The Greenhouse Gas Removal Potential of Bioenergy with Carbon Capture and Storage (BECCS) to Support the UK's Net-Zero Emission Target, Biomass Bioenergy In Press, 2021.

[114] W. Huang, X. Jiang, G. He, X. Ruan, B. Chen, A.K. Nizamani, X. Li, X. Wu, W. Xiao, A novel process of H2/CO2 membrane Separation of Shifted Syngas Coupled with Gasoil Hydrogenation, 5 8, 2020, p. 590.

[115] S.E. Hosseini, B. Butler, An overview of development and challenges in hydrogen powered vehicles, Int. J. Green Energy 17 (1) (2020) 13–37.

[116] BEIS, Digest of UK Energy Statistics (DUKES), Energy, Department for Business, Energy and Industrial Strategy - UK Government, 2020.

[117] J. Radcliffe, D. Murrant, A. Joshi, Roadmap for Energy Storage Research and Innovation, 2020. https://ukesr.supergenstorage.org/.

[118] DEFRA, Farming Statistics, Provisional Arable Crop Areas, Yields and Livestock Populations at 1 June 2020 United Kingdom, 2020.

[119] V. Masson-Delmotte, P. Zhai, A. Pirani, S.L. Connors, C. Péan, S. Berger, N. Caud, Y. Chen, L. Goldfarb, M.I. Gomis, M. Huang, K. Leitzell, E. Lonnoy, J.B. R. Matthews, T.K. Maycock, T. Waterfield, O. Yelekçi, R. Yu, B. Zhou, Climate Change 2021: the Physical Science Basis. Contribution of Working Group I to the Sixth Assessment Report of the Intergovernmental Panel on Climate Change, IPCC, 2021.

[120] G. Lomax, T.M. Lenton, A. Adeosun, M. Workman, Investing in negative emissions, Nat. Clim. Change 5 (6) (2015) 498–500.

[121] S. Searle, C. Malins, A reassessment of global bioenergy potential in 2050, GCB Bioenergy 7 (2) (2015) 328–336.

[122] C.L. Williams, T.L. Westover, R.M. Emerson, J.S. Tumuluru, C. Li, Sources of biomass feedstock variability and the potential impact on biofuels production, BioEnergy Res. 9 (1) (2016) 1–14.

[123] A. Colantoni, M. Villarini, D. Monarca, M. Carlini, E.M. Mosconi, E. Bocci, S. Rajabi Hamedani, Economic analysis and risk assessment of biomass gasification CHP systems of different sizes through Monte Carlo simulation, Energy Rep. 7 (2021) 1954–1961.

[124] M.K. Cohce, M.A. Rosen, I. Dincer, Efficiency evaluation of a biomass gasification-based hydrogen production, Int. J. Hydrogen Energy 36 (17) (2011) 11388–11398.

[125] C. Gough, S. Garcia-Freites, C. Jones, S. Mander, B. Moore, C. Pereira, M. Röder, N. Vaughan, A. Welfle, Challenges to the use of BECCS as a keystone technology in pursuit of 1.5°C, Global Sustain. 1 (2018) e5.